AFRL-RD-PS-
TR-2008-1046

HIGH VOLTAGE FLUX COMPRESSION GENERATORS

Donna M. Chato
Jay B. Chase
Gerald F. Kiutu

CARE'N LLC
12137 Midway Drive
Tracy, CA 95377

2 April 2008

Final Report

AIR FORCE RESEARCH LABORATORY
Directed Energy Directorate
3550 Aberdeen Ave SE
AIR FORCE MATERIEL COMMAND
KIRTLAND AIR FORCE BASE, NM 87117-5776

DTIC Copy

NOTICE AND SIGNATURE PAGE

Using Government drawings, specifications, or other data included in this document for any purpose other than Government procurement does not in any way obligate the U.S. Government. The fact that the Government formulated or supplied the drawings, specifications, or other data does not license the holder or any other person or corporation; or convey any rights or permission to manufacture, use, or sell any patented invention that may relate to them.

This report was cleared for public release by the Office of Public Affairs, 377th ABW, for the Air Force Research Laboratory, Phillips Research Site, and is available to the general public, including foreign nationals. Copies may be obtained from the Defense Technical Information Center (DTIC) (http://www.dtic.mil).

AFRL-RD-PS-TR-2008-1046 HAS BEEN REVIEWED AND IS APPROVED FOR PUBLICATION IN ACCORDANCE WITH ASSIGNED DISTRIBUTION STATEMENT.

//Signed//	//Signed//
TYRONE C. TRAN, DR-II	THOMAS A. SPENCER, DR-IV
Project Manager	Chief, High Power Microwave Division

This report is published in the interest of scientific and technical information exchange, and its publication does not constitute the Government's approval or disapproval of its ideas or findings.

REPORT DOCUMENTATION PAGE

Form Approved
OMB No. 0704-0188

1. REPORT DATE *(DD-MM-YYYY)*	2. REPORT TYPE	3. DATES COVERED *(From - To)*
02-04-2008	Final Report	02 Aug 2007 – 31 Jan 2008

4. TITLE AND SUBTITLE

High Voltage Flux Compression Generators

5a. CONTRACT NUMBER
FA9451-07-M-0088

5b. GRANT NUMBER

5c. PROGRAM ELEMENT NUMBER
65502F

6. AUTHOR(S)
Donna M. Chato
Jay B. Chase
Gerald F. Kiuttu

5d. PROJECT NUMBER
3005

5e. TASK NUMBER
DR

5f. WORK UNIT NUMBER
BL

7. PERFORMING ORGANIZATION NAME(S) AND ADDRESS(ES)

CARE'N LLC
12137 Midway Drive
Tracy, CA 95377

8. PERFORMING ORGANIZATION REPORT NUMBER

9. SPONSORING / MONITORING AGENCY NAME(S) AND ADDRESS(ES)

Air Force Research Laboratory
3550 Aberdeen Ave SE
Kirtland AFB, NM 87117-5776

10. SPONSOR/MONITOR'S ACRONYM(S)
AFRL/RDHP

11. SPONSOR/MONITOR'S REPORT NUMBER(S)
AFRL-RD-PS-TR-2008-1046

12. DISTRIBUTION / AVAILABILITY STATEMENT

APPROVED FOR PUBLIC RELEASE; DISTRIBUTION IS UNLIMITED.

13. SUPPLEMENTARY NOTES
Care'n LLC, the contractor of this SIBR contract, does not claim any proprietary and data rights. The contractor has requested that this technical report to be public releasable.

14. ABSTRACT
Helical magnetic flux compression generators (HFCGs) have been in use for about five decades. There remain limitations to their performance. Recently and for the first time, calculations of high accuracy of HFCG output have been made. The calculated results assume that there are no electrical breakdowns in the generator resulting in a decrease of flux delivered. It has been very difficult to build high-performance generators within desired size constraints as a result. The goal of the Phase I effort is to be able to design and build HFCGs that can operate at higher voltages than are presently achieved. Reaching this goal has required the development of advanced computational tools that allow the calculation of all the vector components of both the electrostatic and inductive internal electric fields within the generators, and identification and understanding of the primary reason, or reasons, for field-induced breakdown.

Using the two existing 2D codes, FlexPDE and CALE, calculations were completed on the constant pitch region of a HFCG and the results incorporated into CAGEN. We have achieved our goals: the complete inclusion in the model code CAGEN for predicting the electric fields within an explosively powered helical flux compression generator. We accomplished this task by using purely two-dimensional physics equation solutions from the trademarked code FlexPDE.

15. SUBJECT TERMS
flux compression generators, magnetocumulative generators, FCGs, MCGs, HFCGs, explosive pulsed power

16. SECURITY CLASSIFICATION OF:			17. LIMITATION OF ABSTRACT	18. NUMBER OF PAGES	19a. NAME OF RESPONSIBLE PERSON
a. REPORT	b. ABSTRACT	c. THIS PAGE			Tyrone C. Tran
Unclassified	Unclassified	Unclassified	SAR	50	19b. TELEPHONE NUMBER *(include area code)*

Standard Form 298 (Rev. 8-98)
Prescribed by ANSI Std. 239.18

This Page Intentionally Left Blank

TABLE OF CONTENTS

LIST OF FIGURES

LIST OF FIGURES (Continued)

LIST OF FIGURES (Continued)

Figure Page

LIST OF FIGURES (Concluded)

LIST OF TABLES

This Page Intentionally Left Blank

1.0 SUMMARY

Although helical magnetic flux compression generators (HFCGs) have been in use for about five decades, there are still limitations to their performance that are not fully understood. Major advances have occurred over the last few years that allow, for the first time, calculation of their output with high accuracy. However, the calculated results assume that there are no electrical breakdowns in the generator. When breakdowns do occur, there is usually a decrease of flux delivered to the generator load. Practically, this means that HFCGs must be operated at less stressing values of maximum output voltage, peak dI/dt, gain, or initial flux; or, they must be increased in size to prevent breakdown for desired output characteristics. Because of this, it has generally been very difficult, or even impossible, to build high-performance generators within desired size constraints, or it means that output currents cannot be delivered to loads in as short a time period as desired or required.

The goal of the Phase I effort is to be able to design and build helical flux compression generators that can operate at higher voltages than at present, and therefore meet the demands for either compactness or output voltage. Achievement of this goal has required the development of advanced computational tools that allow the calculation of all the vector components of both the electrostatic and inductive internal electric fields within the generators, and identification and understanding of the primary reason, or reasons, for field-induced breakdown.

Using the two existing 2D codes, FlexPDE and CALE, calculations were completed on the constant pitch region of a HFCG. In addition, an approach using a Biot-Savart technique is being developed and will provide a fully three-dimensional evaluation of the electric fields in this system. After incorporating the enhancement factors discussed above, calculations on CAGEN have been completed for three example helical flux compression generators (HFCG). The first is the original HFCG that acted as the baseline for the project. It was called HGWL1. It is quite small, only 80 mm in diameter, and is a model of an HFCG that electrically broke down. The second, called HHT79, is a very large HFCG, more than 300 mm in diameter, and it did not break down. The third HFCG is called JAKE and is 170 mm in diameter. It has been known to break down electrically, but the results of an experiment are not available.

All three of the included examples, HGWL1, HHT79, and JAKE, use insulation around the wires used for the stator winding. Some use layers of insulation layered against the cylindrical inside surface of the windings, as well. All three of these HFCG designs use gaseous SF_6 at one atmosphere of pressure to fill the volume between the armature and the stator. Consequently, knowing the electric field strength everywhere within the HFCG will not, by itself, determine the probability of electrical breakdown. There are generally accepted danger zones. For example, in dry air one would expect breakdown to occur at about 1 kV/mm, while in one atmosphere of SF_6that value might be as much 4 kV/mm, and most common solid insulators begin to break at 20 kV/mm. However, with the knowledge of how large and where the electric field maxima are located, for systems with similar materials, predictions can begin to be made. This work provides the first of the set of knowledge that is required. This work enables the prediction of the electric field structure.

We have achieved the last of our goals: the complete inclusion in the model code CAGEN for predicting the electric fields within an explosively powered helical flux compression generator. We accomplished this task by using purely two-dimensional physics equation solutions from the trademarked code FlexPDE.

The development of the 3D helical model has been pursued with the notion that some benchmarking of the three dimensional limitations to our models would be wise. However, nothing was developed within the time span of the project lifetime.

2.0 INTRODUCTION AND BACKGROUND

Although helical magnetic flux compression generators (HFCGs) have been in use for about five decades, there are still limitations to their performance that are not fully understood. Major advances have occurred over the last few years that allow, for the first time, calculation of their output with high accuracy [1-4]. However, the calculated results assume that there are no electrical breakdowns in the generator. When breakdowns do occur, there is usually a decrease of flux delivered to the generator load. Practically, this means that HFCGs must be operated at less stressing values of maximum output voltage, peak dI/dt, gain, or initial flux; or, they must be increased in size to prevent breakdown for desired output characteristics. Because of this, it has generally been very difficult, or even impossible, to build high-performance generators within desired size constraints, or it means that output currents cannot be delivered to loads in as short a time period as desired or required.

Typically, the estimated electric fields in generators are substantially below the ambient breakdown strength of the insulating gas, even using sulfur hexafluoride (SF_6), which is about 2-3 times better than air. Some researchers have established empirical operation constraints in terms of maximum equivalent source voltage (i.e., $V_s = -(dL/dt)I$) [5] for a particular generator design, initial current, and load, but these are only approximate and don't scale to different designs, making them limited in their utility. The consequence of this inability to gauge the maximum operating parameters is that, at the very least, multiple iterations of experiments must be performed to establish the limits, and in the worst case, the design must be scrapped entirely when it can't perform up to specifications. We emphasize that it is electric fields, not voltage, that cause breakdown.

2.1 TECHNICAL OBJECTIVES

The technical objectives for the Phase I effort are rather straightforward. The goal is to be able to design and build helical flux compression generators that can operate at higher voltages than at present, and therefore meet the demands for either compactness or output voltage.

Achievement of this goal has required the development of advanced computational tools that allow the calculation of all the vector components of both the electrostatic and inductive internal electric fields within the generators, and identification and understanding of the primary reason, or reasons, for field-induced breakdown.

It was conjectured that the gas within the FCG might be playing an important role in the electric field breakdown due to its motion through the magnetic field. It has been subsequently found that this concern is unnecessary. As will be seen, sufficient field strength is found by other, more geometry related, means.

2.2 TECHNICAL ISSUES

One of the fundamental reasons that HFCG operational limits cannot be determined and optimized is that all of the electric fields in the system must be calculable, and there are no good tools for calculating the fields in the actual, three-dimensional geometries of these devices. Furthermore, researchers have generally only been able to calculate electrostatic fields (i.e., derivable from a scalar potential $\vec{E}_e = -\vec{\nabla}\varphi$). The inductive component of the electric field, which results from changing magnetic fields, can also be important. We have developed techniques for calculating the inductive electric fields in two dimensions by calculating the magnetic vector potential in 2D. As can be seen in any standard electromagnetism text, the inductive electric field is just $-d\vec{A}/dt$, where $\vec{A}$ is the magnetic vector potential, and the appropriate gauge condition has been applied. Although we can calculate the inductive fields from the magnetic vector potential when the fields are only inductive, the fields are, in general, a combination of

electrostatic and inductive. Furthermore, we know that the electric breakdown threshold along the surface (tangential field component) of a dielectric is usually much lower than the bulk breakdown strength, so it is important to know the direction of the field at dielectric interfaces.

The range of HFCG operating voltages has been found empirically to be well below the ranges one would expect for laboratory pulsed power devices that use standard solid and gas dielectric insulation. The typical maximum output terminal voltage for megajoule-class HFCGs is approximately 50 kilovolts, corresponding to an internal equivalent internal source voltage of approximately 160 kV. For typical armature-stator gaps of 8 cm, the maximum output voltage (approximately 50 kV) represents a maximum electric field stress of only 6 kV/cm, while the internal average radial electric field, at the axial location of the maximum value, is approximately 20 kV/cm. Since the breakdown strengths of air and SF_6 at standard temperature and pressure (STP) conditions are approximately 30 kV/cm and 100 kV/cm, respectively, the question naturally arises, "How can breakdown occur at such low field values?"

We had hypothesized that magneto-hydrodynamic (MHD, or $\vec{v} \times \vec{B}$) action could lead to much higher field values. There are three characteristic speeds in the generator: the armature radial expansion speed, the high explosive (HE) detonation speed, and the armature-stator helical contact speed. Clearly, the fill gas is pushed, radially outward, ahead of the armature, slightly faster than the armature expansion speed (of order 2 mm/μs). Typical HE detonation speeds, which are also the speed at which the self-similar expanding armature cone moves axially, are on the order of 8 to 9 mm/μs. Characteristic maximum magnetic flux density values in HFCGs are typically less than 100 T (1 MG), by design, to avoid unintended conductor motion, melting, or vaporization. Therefore, the radially moving gas ahead of the expanding armature can experience an MHD electric field as high as 2 kV/cm, and it is directed primarily in the azimuthal direction. The axial motion ahead of the intersection of the contact point can increase this value to approximately 8 kV/cm. Both of these estimated field values are still below the dielectric strength of the fill gas at *ambient* conditions. Although compression and heating of the gas will occur, at least for SF_6 these conditions should still allow a breakdown strength higher than the electric fields experienced by the gas. At elevated temperatures, SF_6 dissociates, but the dissociated molecules, SF_5 and SF_4, are even better insulators than SF_6 (we have not addressed the issue of photo-ionization here).

As the armature expands and contacts the stator windings, there is some possibility that a component of gas acceleration could be in the contact velocity direction. The (primarily azimuthal) contact speed is given approximately by the product of detonation speed and the ratio of stator underside circumference to pitch, $\vec{v}_c = \vec{v}_\Delta (2\pi r_s / p)$. For a typical circumference-to-pitch ratio of, say, 20, the corresponding contact speed is approximately 200 mm/μs, and using the characteristic peak magnetic field value of 0.5 MG, this conjectured peak MHD electric field of 100 kV/cm, which exceeds the nominal breakdown strength of even SF_6; and, the direction of the field is poloidal rather than toroidal, which can lead to either turn-to-turn stator breakdown or stator-to-armature breakdown!

The viscous fluid Reynolds number of the SF_6 is much greater than one in the operating HFCG. Consequently, any flow disturbance will grow extremely rapidly into fully mixed turbulence. There will always be, in these circumstances, some portion of the fluid that has very fast rotational speeds and some small amount of the fluid may exhibit instantaneous speeds reaching values above 100 mm/μs. So it is possible that this mechanism can also account for electric field stresses above the break down limit for accelerated gas field and the direction of this stress would be, at moments, in a radial direction making breakdown possible.

The best available equation of state and conductivity model for sulfur hexafluoride is in the literature (we note that Los Alamos National Laboratory has dealt with this problem in calculating the performance of

the Ranchero flux compression generator [6], so that there may be an SF_6 EOS model available from there). A critical issue is that the literature indicates that SF_6 becomes liquid-like during the rapid compression experienced inside the HFCG. Using the 2D magneto-hydrodynamics code CALE, the various components of peak velocity of the gas motion were to be assessed and the resulting electric field stresses determined. Applying the K-E turbulence theory to the gas field, estimates for the turbulent speeds and directions were to be ascertained along with the concomitant electric stress. However, as we proceeded with this project, we discovered that we did not need to pursue these topics.

2.3 APPROACH BACKGROUND

We have developed a technique for calculating the total (electrostatic plus inductive) electric fields using electric vector potentials [7]. We know of no other convenient means of performing such calculations. A simple derivation and representative results of the technique are given here. We begin with Poisson's equation in the absence of space charge,

$$\vec{\nabla} \cdot \vec{D} = 0 . \tag{1}$$

If the divergence of a vector is identically equal to zero, then it can be represented as the curl of another vector, so we express the electric flux density as the curl of an electric vector potential, $\vec{F}$:

$$\vec{D} = -\vec{\nabla} \times \vec{F} . \tag{2}$$

We now express the electric field in terms of the electric vector potential using the constitutive relation,

$$\vec{D} = \varepsilon \vec{E} : \tag{3}$$

$$\vec{E} = -\left(\vec{\nabla} \times \vec{F}\right) / \varepsilon . \tag{4}$$

Next, we use Faraday's Law,

$$\vec{\nabla} \times \vec{E} = -\frac{\partial \vec{B}}{\partial t} ; \tag{5}$$

substituting for $\vec{E}$ from Eq. (4), we finally obtain

$$\vec{\nabla} \times \left(\vec{\nabla} \times \vec{F} / \varepsilon\right) = \frac{\partial \vec{B}}{\partial t} . \tag{6}$$

This vector Poisson-type equation is readily solvable in two dimensions using various partial differential equation (PDE) solvers, such as FlexPDE™. As an example, we show below the solution for an annular superconducting cavity with two different insulating materials fed by a voltage source [7]. In this case, the electric fields are purely inductive, and cannot be found using standard electrostatic field solvers. Figure 1 shows the electric field streamlines, which give the direction of the field. Figure 2 shows the relative magnitude of the electric field, and figure 3 shows contours of the corresponding electric vector potential.

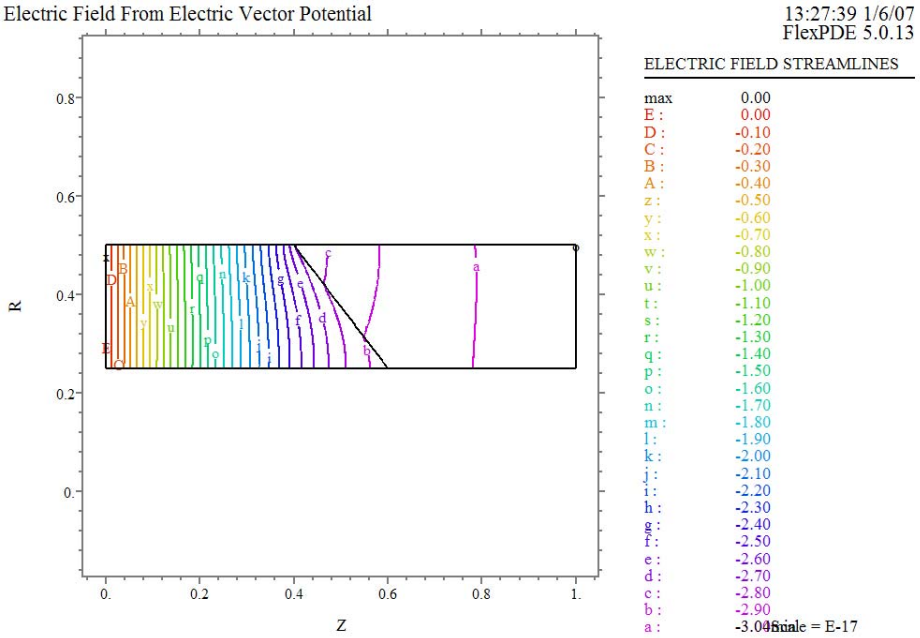

Figure 1. Electric field streamlines derived from the electric vector potential for an annular superconducting cavity with two different dielectric materials.

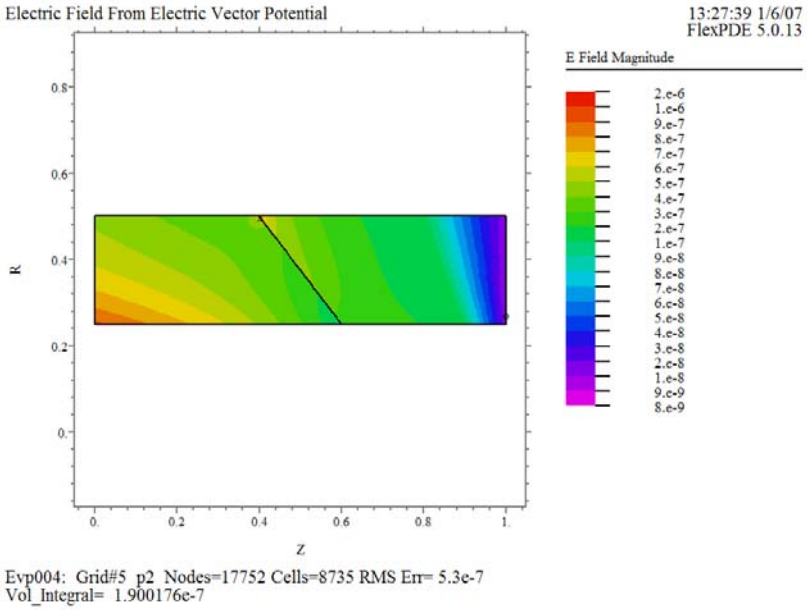

Figure 2. Relative amplitude of the electric field derived from the electric vector potential.

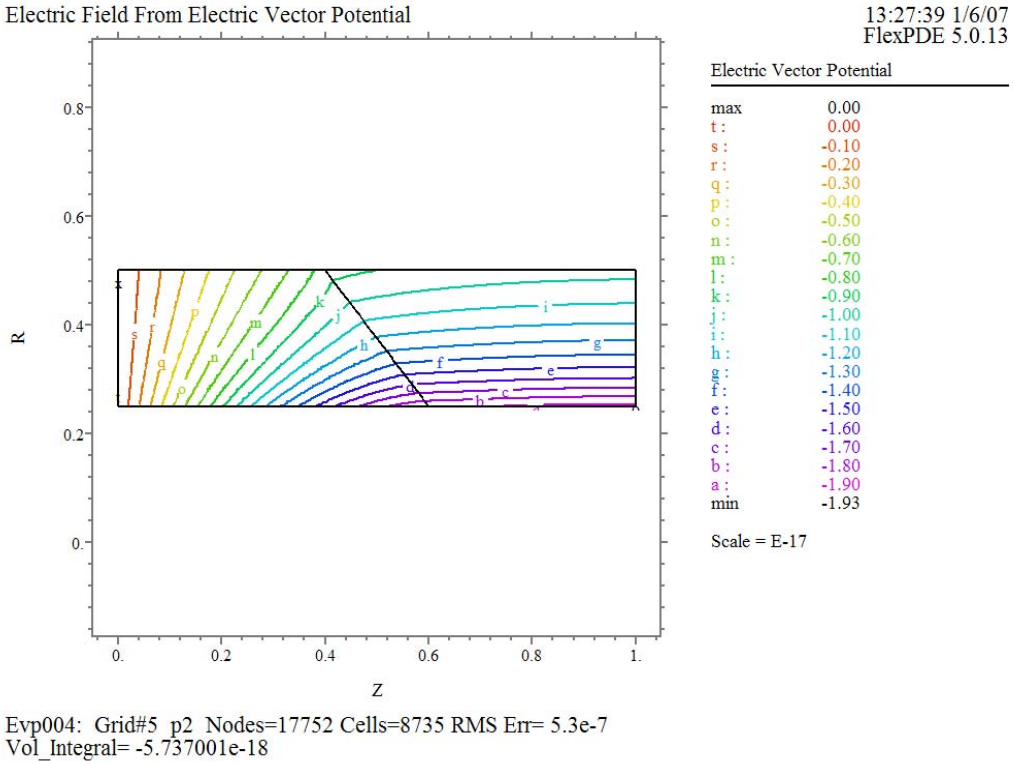

Figure 3. Contours of the electric vector potential.

This technique is most useful for poloidal total electric field calculations, since the source term in Eq. (6) is known for axi-symmetric problems:

$$B_\varphi(r,t) = \frac{\mu_0 I(t)}{2\pi r}. \tag{7}$$

The toroidal magnetic fields for HFCGs are nearly axi-symmetric.

For toroidal (inductive) electric fields in nearly axi-symmetric geometries, it is more convenient to solve, in 2D (*z*,*r* plane), for the magnetic vector potential normalized to the current. Then, the inductive electric field is given by

$$E_\varphi = -\frac{\partial A_\varphi}{\partial t}. \tag{8}$$

The result of such a calculation for a one-turn section of an infinitely long, high-conductivity coil with coaxial interior cylindrical conductor is shown in Fig. 4.

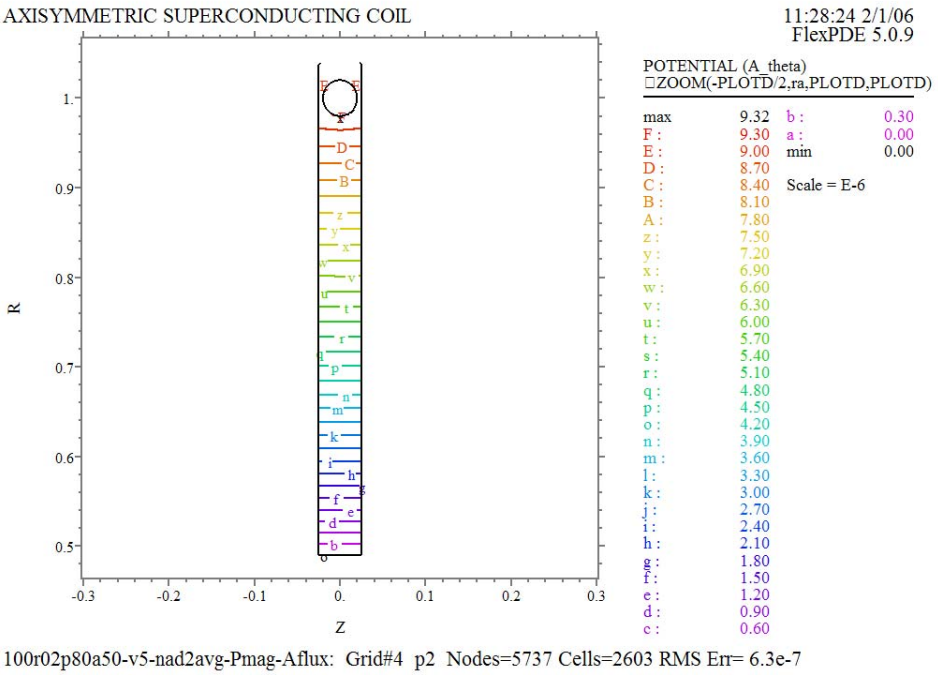

Figure 4. Normalized inductive electric field for an infinitely long, high-conductivity coil surrounding a coaxial conductor at half radius.

In this case, the electric field (and vector potential) increases nearly linearly from the inside conductor to the coil, since the (primarily) axial magnetic field is nearly uniform, and we know that for the axi-symmetric case,

$$A_\varphi(r,t) = \frac{\psi_p(t)}{2\pi r} \approx \frac{nI(t)}{2}\left(r - \frac{a^2}{r}\right), \tag{9}$$

where ψ_p is the poloidal magnetic flux, n is the coil linear turns density (inverse pitch), and a is the radius of the interior conductor.

The Care'n LLC uses the 2D Lawrence Livermore National Laboratory MHD code, CALE, to

perform both hydrodynamic and full MHD calculations. It is a well known, well benchmarked, and widely used code by the physics research community. It has HE detonation physics, material strength in the form of the Steinberg-Guinan model, and a variety of material EOS and electrical conductivity models.

In Figures 5 and 6 we show preliminary results of a calculation of gas motion ahead of a conical HFCG armature impinging on an outer cylinder. For this calculation, an over-simplified gas EOS was used, but it illustrates the type of hydrodynamic calculation that can be performed. Figure 5 shows the computational mesh and color contours of pressure near the armature-stator contact point. Figure 6 shows color contours of material density, upon which are superimposed material velocity vectors.

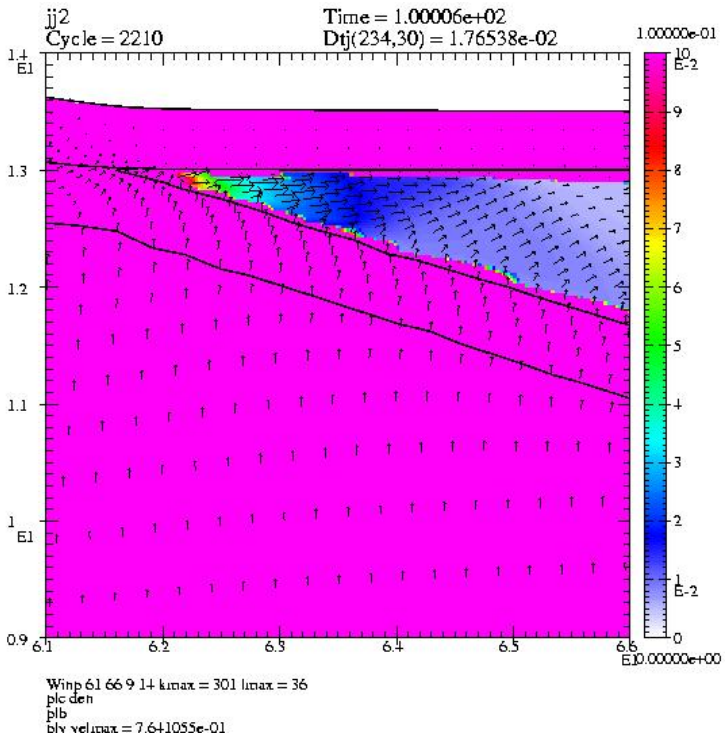

Figure 5. Computational mesh and pressure color contours from a preliminary CALE calculation to determine gas motion ahead of an HFCG armature impinging on a cylindrical stator.

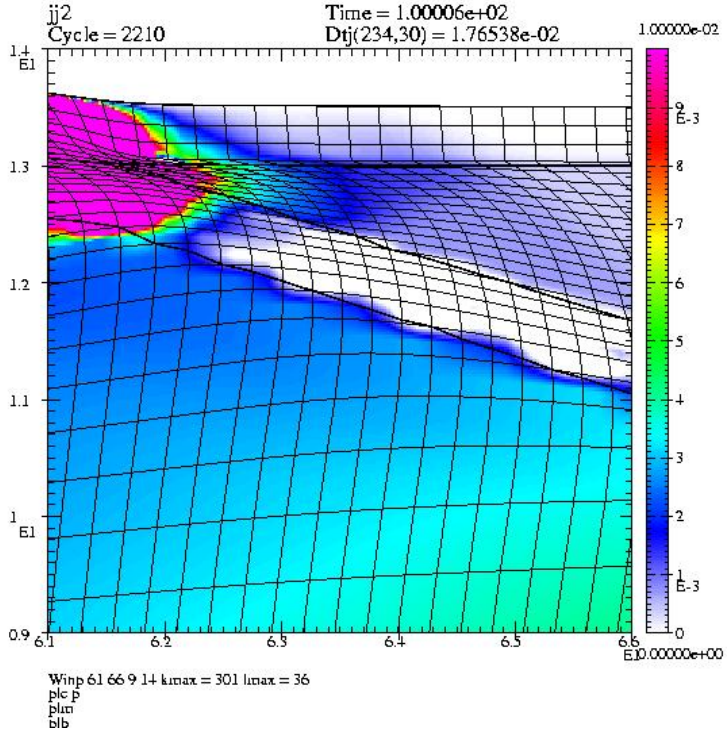

Figure 6. Material velocity vectors superimposed on color contours of material density from a preliminary CALE calculation.

The 1½-D model computational tool we use to calculate the performance of HFCGs is the Care'n Company proprietary code, CAGEN [2-4,8-13]. It has been under almost continuous development for nearly 25 years by the principle Members of The Care'n LLC. CAGEN consists of models for the operation of the HFCG itself, along with models to self-consistently include complex load circuits composed of inductors, fully nonlinear resistors, switches, fuses, capacitors, and transformers. The portion of CAGEN of interest for this proposal is just the HFCG.

CAGEN includes the effects of nonlinear diffusion into the metal parts, magnetic pressure acceleration of the metal parts, and variable-pitch and bifurcated winding patterns. It has built-in material equation of state data, with provision to incorporate custom data. These attributes have made it possible to design HFCGs whose experimental performance has not differed significantly from that calculated by the code. Within the last two years, two models were added to CAGEN that have made the use of empirical tuning factors, or "fudge factors," such as those in virtually every other code, no longer necessary. These models are the Kiuttu Contact Resistance Model (KCRM) [1,2] and the Kiuttu Proximity Effect Model (KPEM) [3,4]. Incorporating these two models has obviated the need for any adjustable parameters to quite accurately model an enormous range of HFCGs. Several conference papers have been presented discussing these advances over the last two years, and the originator of the models was invited to summarize these accomplishments at the Megagauss 2006 international conference held in Santa Fe, NM, in November of 2006 [3]. We emphasize that *CAGEN is the only known FCG modeling code that can accurately calculate the performance of helical flux compression generators without using empirical tuning factors*.

CAGEN could not, prior to this work, accurately predict the internal electric field stresses during the operation of an HFCG. It is those stresses that limit the ability of reliable, robust designs to approach conditions near the internal voltage breakdown threshold. We have extended the electric field calculations described above to cover HFCGs over practical design ranges, and incorporated the results into CAGEN. CAGEN now provides calculations of internal electric fields, making predictable, reliable designs possible.

2.4 TASK OUTLINE

I. Evaluate issues
   A. Evaluate the experimental database for information leading to choosing the correct theoretical approach.
   B. Extend electric and magnetic vector potential methodologies to calculate all components of electric fields for HFCGs
      1. r,ϕ,z vector components
      2. Electrostatic and inductive components
   C. If the above E fields are insufficient to explain the existing data base, move forward by finding the best equation of state and conductivity model for sulfur hexafluoride, by performing CALE hydrodynamic calculations to determine the peak velocities reached in the SF_6 gas, and by doing CALE MHD calculations to estimate the peak $\vec{v} \times \vec{B}$ electric fields in SF_6 gas. Subsequently, of course, step C was found to be unnecessary, and therefore the conjecture upon which step C was based, is probably wrong.

II. Incorporate the results into the CAGEN code.

III. Perform advanced analysis using CAGEN and auxiliary calculations to quantitatively assess the relative importance of issues and the means of mitigating them.

IV. In a Phase II contract, Care'n LLC will execute a large number of quite simple HFCG experiments, with the goal of establishing validation of the models put into CAGEN.

3.0 THEORY DEVELOPMENT

Three regions of a HFCG were identified: the contact point, the more-or-less constant pitch center region, and the bifurcations. It was decided to focus on the constant pitch region. The contact point and the bifurcations seem not very relevant because the high voltage breakdowns are not observed to take place there. Symmetry considerations have made it clear that all three components of the E field are contributed to by both the resistive nature of the conductors (electrostatic) and the time rate of change of the magnetic field (inductive) in the vicinity of the conductors. These field component magnitudes all exhibit enhancement as one examines points nearer the conductor surfaces.

Since there exists, in theory, a conformal map that converts the constant pitch helix with constant radius armature inside, intrinsically 3D problem, to a 2D problem. Consequently, a reasonably accurate and quantitative evaluation of the E field components should be available via 2D approximations. These results must be generated for a range of several parameters. The procedure included first treating the conductors as superconductors, then conducting but limiting the resistivity to a constant value (linear)

and finally treating the conductors as real with full variable resistivity (nonlinear).

Using the two existing 2D codes, FlexPDE and CALE, calculations were completed on the constant pitch region of a HFCG. In addition, an approach using a Biot-Savart technique is being developed and will provide a fully three-dimensional (3D) evaluation of the electric fields in this system. We have achieved two-dimensional (2D) maps of the electric field for a helical generator fired by SAIC for the AFRL. This generator electrically broke down, and we can now suggest the reason. The time rate of change of the magnetic field in the device is the source of the inductive electric fields, and they are directed in the theta direction in the 2D approximation. The electrostatic field components that are due to the material resistance and the material motion in the magnetic field (V X B) are directed in the R and Z directions in the 2D approximation.

The vector field exhibits enhancement over the average field as one considers points close to the conductor surfaces. It is the proper vector combination of the inductive and static electric fields along with the electric field due to the motion of the armature that will determine whether the subject system will break down electrically. Consequently, all of these field components must be computed.

The subject helical flux compression generator (HFCG) is called the HGWL and has been fired several times. Two such firings, using identical geometric features differed only by the amount of injected current used to start the generating action. Number 4 used 3.17 kA and broke down, while number 5 used 1.588 kA and did not. This generator is quite suitable for this 2D analysis because:

- the angle between the armature and the stator is very small, ~10.5 degrees, making a model with non-slanting armature viable;
- the conducting materials are all copper, simplifying the model; and finally,
- the geometry of the HFCG is simple.

First, an explanation of the extraction of the time and place of the breakdown in the experiment is needed.

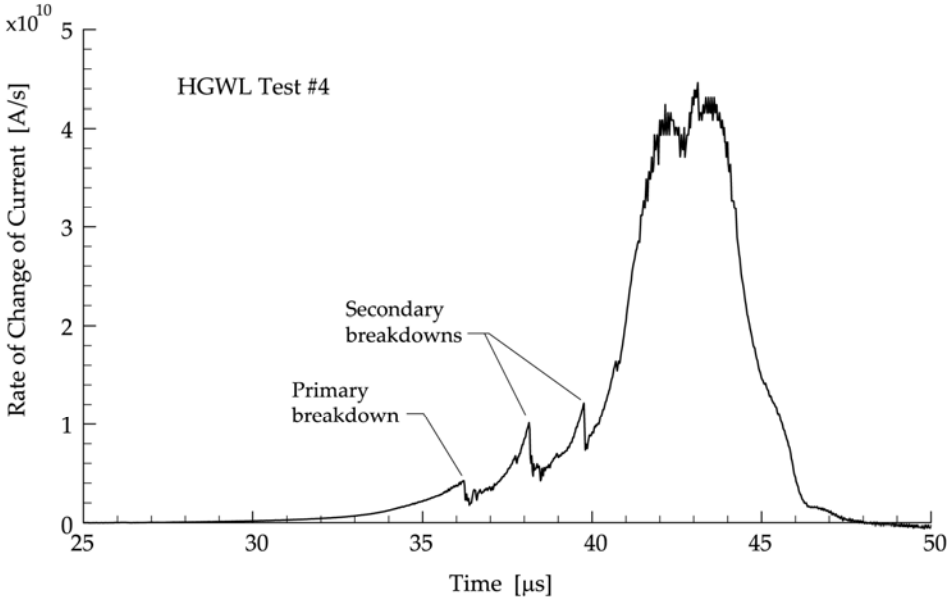

Figure 7. The time derivative of the experimental current is shown with the various moments of breakdown labeled. The figure is taken from a SAIC internal report.

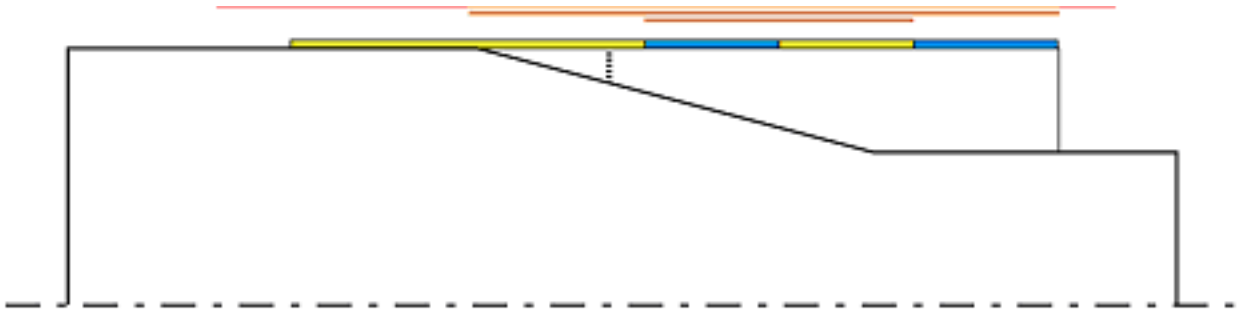

Figure 8. The diagram shows, schematically, the position of the breakdown relative to the first bifurcation in the stator windings. Again, the diagram is taken from the above SAIC internal report.

This analysis consists of first establishing the time for when the armature first contacts the stator windings. This is obtained by careful examination of the early dI/dt curve at a level not shown in figure 7. The time of the breakdown is clear from figure 7, and the speed of the contact point in the axial direction is just the explosive detonation speed (8.311 km/s), so the position of the contact point when the breakdown occurs is apparent. The position of the breakdown path at the same time is less apparent. By noticing, on the dI/dt curve, when the d^2I/dt^2 (the second derivative) recovers to the pre-breakdown value, and assuming this means no physical artifacts of the breakdown remain and that is because the contact point has over-run the position of the breakdown path, we can guess at the position of the breakdown. On figure 7, the time of the break is 36.2±0.2 μs, while the time of recovery is 37.3 μs. This means the position of the break is 21.25 mm downstream from the beginning of the windings, and the position of the contact point between the armature and the stator is 13.8 mm from the beginning of the winding. The

first bifurcation is at 43.5 mm from the beginning of the winding. Again from the experiment, the current just before the break is 10.9 kA, and dI/dt at that time is 4.0E9 A/s.

The remaining information needed for the obtaining the vector electric field must be gotten from the CAGEN modeling code. Locally one must know the resistivity (eta) of both the armature material and the stator material at the time and location of the break. These values are: eta (arm) = 1.755E-6 Ω-cm and eta (stat) = 1.748E-6 Ω-cm. In addition, the current density along the bottom of the wire and the surface of the armature is required. These are: j (arm) = -0.044E7 A/ cm^2, and j (stat)=0.173E7 A/ cm^2. The most important number is the potential difference between the breakdown point on the stator winding and the opposing point on the armature. This number is actually, in terms of magnetic fields, the line integral of the velocity of the moving armature crossed into the magnetic field near the armature. The integral is to be taken from the contact point to the breakdown point along the surface of the armature. The resistive component of the field must be added. The CAGEN model is in terms of the entirely equivalent inductance and resistance of the circuit. Contributions to the inductance and resistance due to axial elements are computed in CAGEN. If these are combined correctly and summed over the axial elements from the contact point to the break point, the voltage required is obtained.

$$V = \sum_c^b \left[\frac{d(L_i I)}{dt} + R_i I \right] DeltaZ_i ,$$ i summed from c to b.

V, computed above, is some fraction of the total source voltage which is defined as:

$$V_s = \frac{dL_{total}}{dt} I .$$

So now to compute the vector electric field components, a 2D representation of the real geometry is used. Instead of a helical winding, a series of loops is used, such that the center-to-center spacing of the loops is just equal to the pitch of the actual helix. Since the breakdown region is more than 7 pitches from the contact point, a periodic boundary condition was used. In this structure, two perfect planes, perpendicular to the axis, are passed through the minor diameter of the two adjacent loops. These planes are the periodic boundaries – it's as if this pattern of two half-loops and the gap between were to be continued to the right and to the left forever. In this approximation, the inductive field is all in the theta direction, and the electrostatic fields are in the R and Z directions, only. For the inductive field component both the code CALE and FlexPDE were used, while only the program FlexPDE was used to generate the R and Z components. The theta electric field component is fairly small, in this case, compared to the other components.

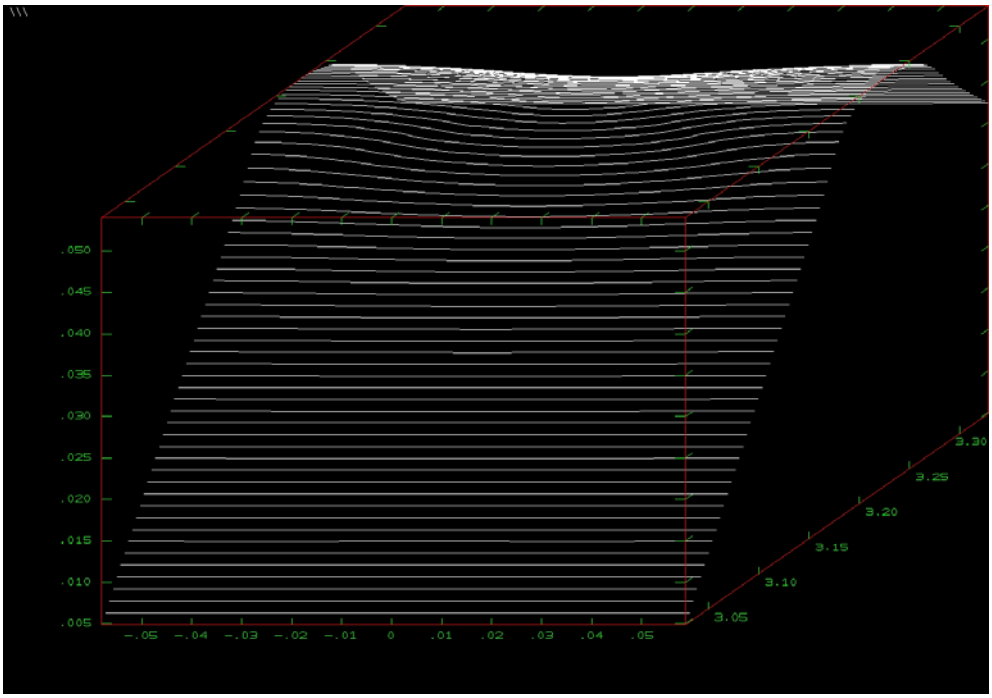

Figure 9. This shows the inductive component of the electric vector field, only in the theta direction. The horizontal axis is distance in the Z or axial direction in centimeters. The center value of zero is exactly between the two wires. The axis extending back into the paper is the radial direction with the armature surface at the very front (bottom). The vertical axis is the electric field magnitude in units of DKV/cm (1.E4 Volts/cm).

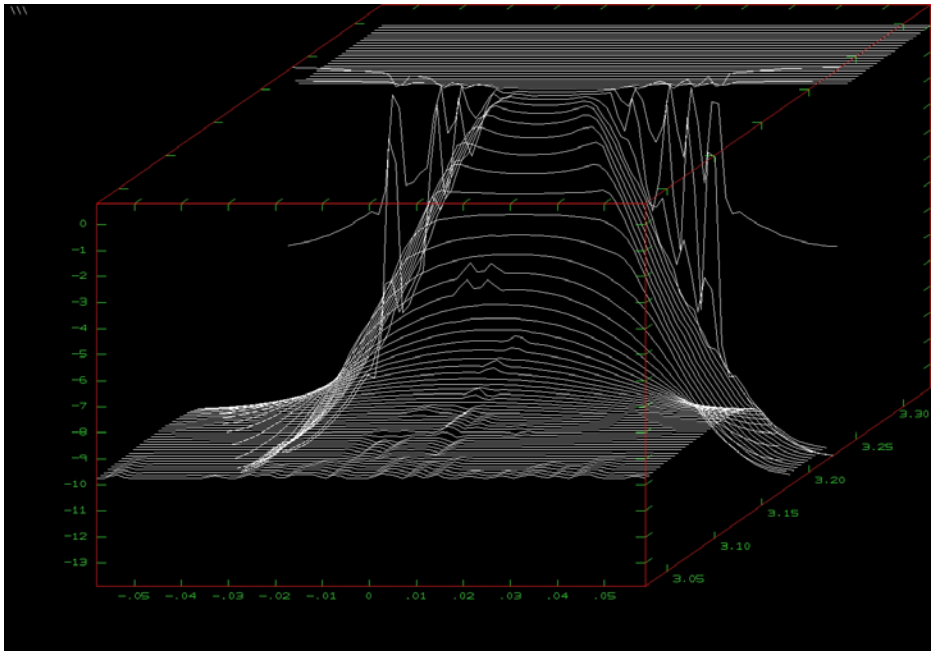

Figure 10. This shows the radial component of the field. The units and axes are defined in figure 9. Note that zero magnitude is at the top of the vertical axis.

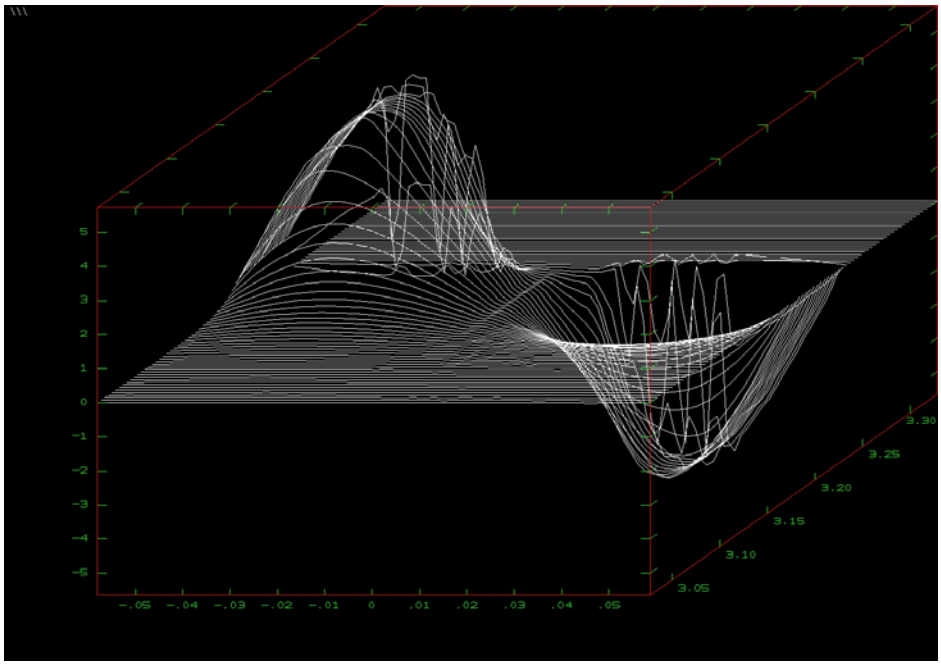

Figure 11. This shows the Z component of the field. The units and axes are defined in figure 9.

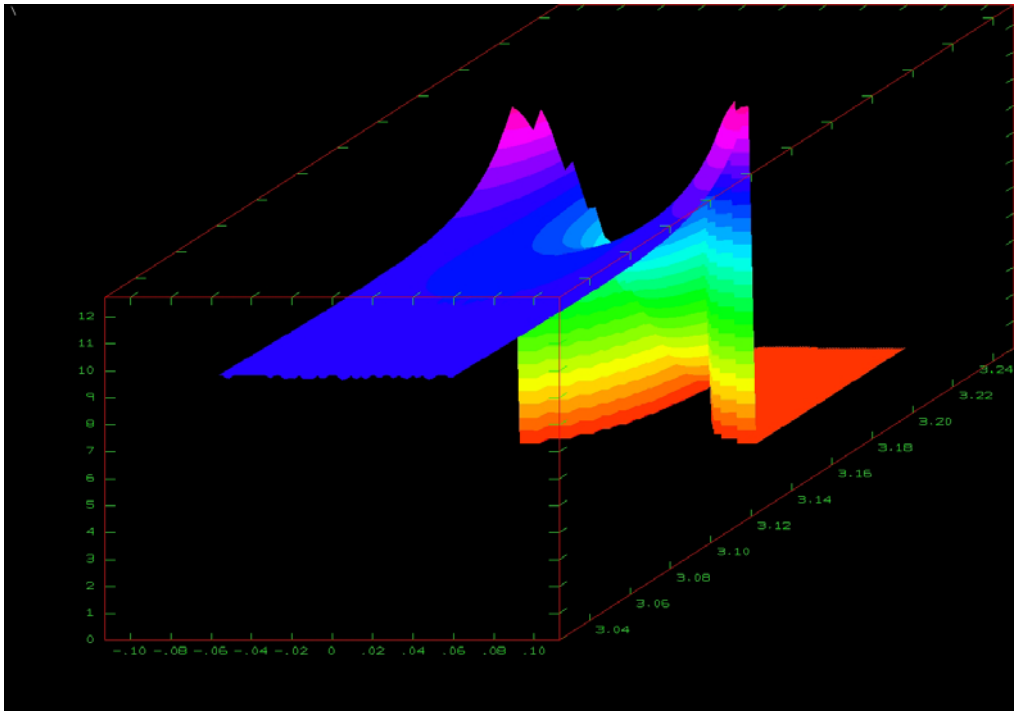

Figure 12. This image is a colored contour plot of the magnitude of the vector field. The same axes and units are used. The purple peaks are located just under the inner surface of the wires and have a magnitude of 127.3 kV/cm.

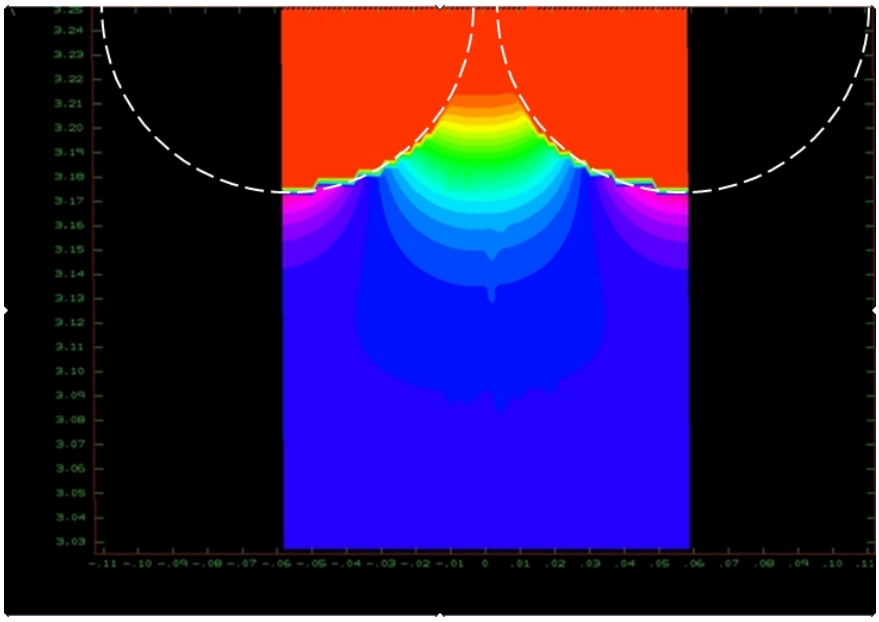

Figure 13. This shows the same as figure 12 but looked at from the top. Now the radial axis is vertical, and the Z-axis is horizontal. The shape of the two half-wires is just visible. Red is near zero, and purple is highest.

The geometry that appears in the above figures can be somewhat difficult to envision. There are two half wires whose diameters are coincident with the right and left edges (in Z) of the figures. Each wire has a minor radius of 0.512 mm and a major radius of 32.262 mm. The armature surface is at a radius of 30.272 mm. The gap between the two wires is 0.151 mm.

The electric fields in an actual HFCG that actually electrically broke down have been computed. The peak electric field magnitude was computed to be 127.3 kV/cm. This position is against the under surface of the wire and buried in solid insulation. We know, however, that solid insulations, depending on type, can break at these field strengths. The enhancement factor is to be defined as the ratio of the actual peak field divided by the average electric field, which is equal to the voltage at the suspect position-time, divided by the radial distance between the stator and the armature. This value is 1.28.

Restating the limitations of these results are of value:

1. The use of 2D loops in place of full 3D helical windings is believed to be a small error, but until a comparison can be made one cannot be sure. That comparison awaits the development of the Biot-Savart technique of solution.
2. The use of periodic representation is believed to create a quite small error, but again until a comparison can be made one cannot be sure.
3. The CALE calculation of the inductive (theta) part needs to be improved to include the appropriate diffusion of magnetic field into the wire. The inductive fields computed by FlexPDE utilize the V X B component from the CAGEN code, and that needs verification.

4. Perhaps as important is the need to compare this theoretical analysis to more of the experiment database. A limited relevant database is available. All such experiments consist of one in which there is an observed electrical breakdown, followed by one for which the current was decreased greatly to insure that no break would subsequently occur. Consequently, no real threshold has ever really been obtained.
5. Finally, the theory needs to be utilized in a variational mode in order to assess the sensitivity of these reported results to dimensional variations, experimental errors, and design variations. Figure 14 shows a very preliminary example of this kind of analysis.

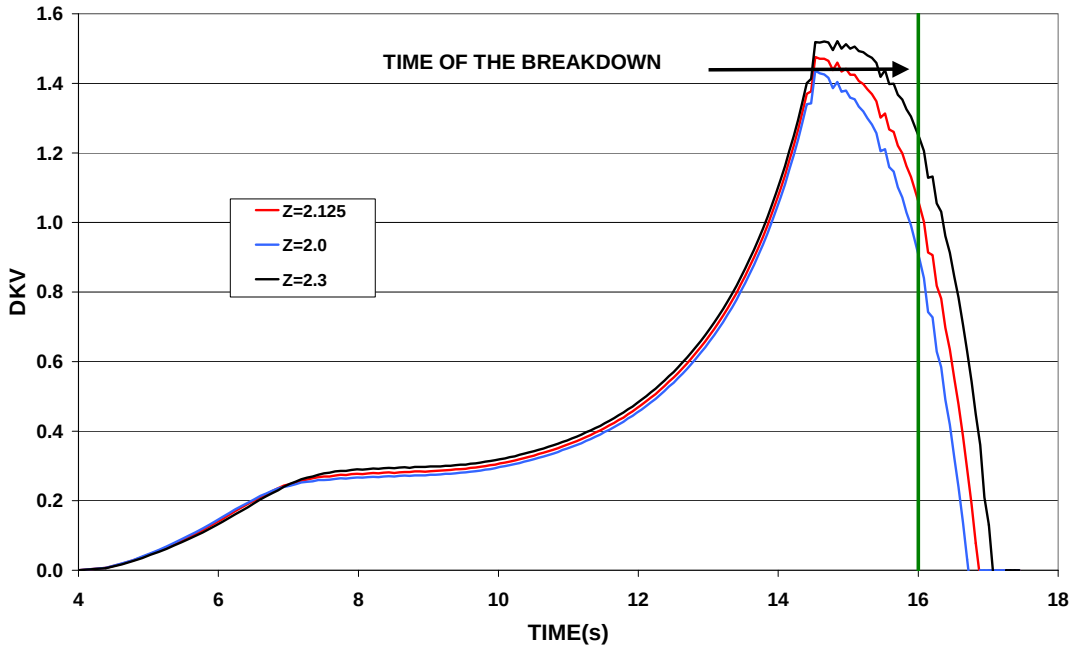

Figure 14. Showing the variation in voltage drop realized by monitoring different positions in the HFCG.

3.1 CHANGE IN APPROACH

The Work Breakdown Structure (WBS) given in the appendix was, at this point, modified. Consequently, elements 1.3.1 were deleted, the required electric field strength to cause breakdown having been found without those questionable issues being studied and included. Instead, we extended the development of the existing theory. The development of the 3D helical model will continue, hopefully to provide some understanding of the limitations of using a 2D approximation. There is a need to understand how the enhancement factor, discussed above, depends upon the geometry of the HFCG such as wire diameter, major diameter, the ratio of the armature diameter to the winding diameter, and more. The last step of the project is to incorporate the theory into the code CAGEN in order to provide an electric breakdown predictive capability for designers.

3.2 CAGEN RE-PROGRAMMING

The changes in CAGEN make it capable of receiving the data generated by the two dimensional calculations done on FlexPDE and CALE. These data have been rendered in the form of "enhancement factors". In this way, when CAGEN calculates an average electric field, a simple multiply yields the peak field.

Various aspects of the average values are shown in the figures 15-23. Figure 15 is shown as a sort of road map for the others. The source voltage is dL/dt times I and is larger in value than any internal voltage can be as it represents the source without any losses. The points A and B give some references. Note that the maximum of the source voltage is just a little larger than 100 KV.

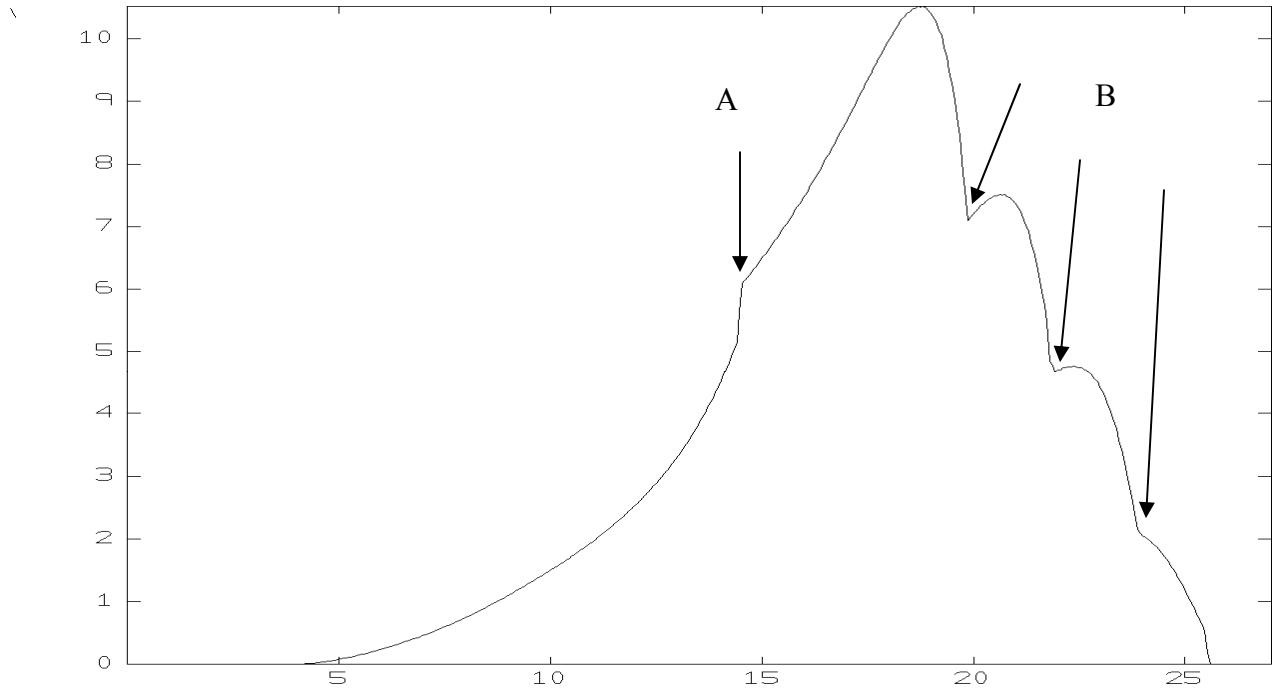

Figure 15. For the HGWL1 problem, this shows the "source voltage" versus time. The units are in DKV (10,000 volts). Point A is the arrival of the armature at the first winding of the stator. Points B are the bifurcations in the FCG winding.

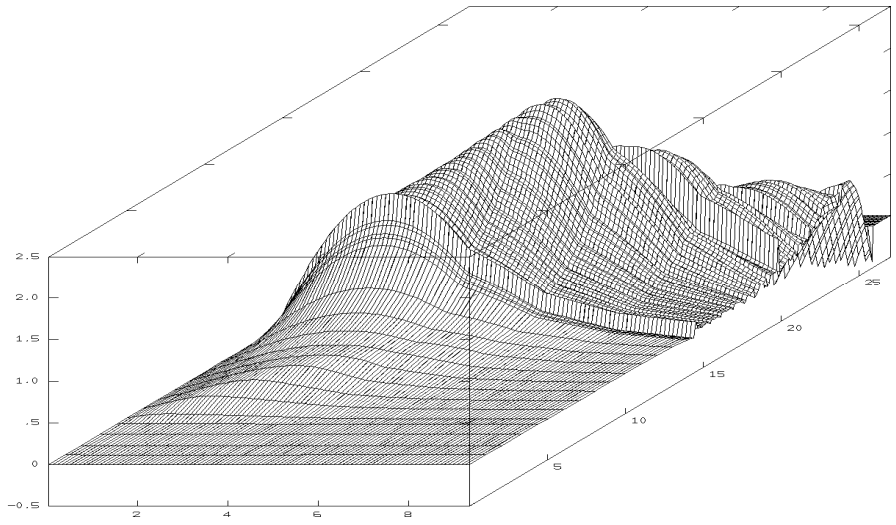

Figure 16. Shows the voltage difference between the stator and the armature. The axis in front (left-right) is the Z position down the axis of the FCG; the vertical axis is the voltage value in DKV (10,000 volts); and the axis into the paper is time in μs.

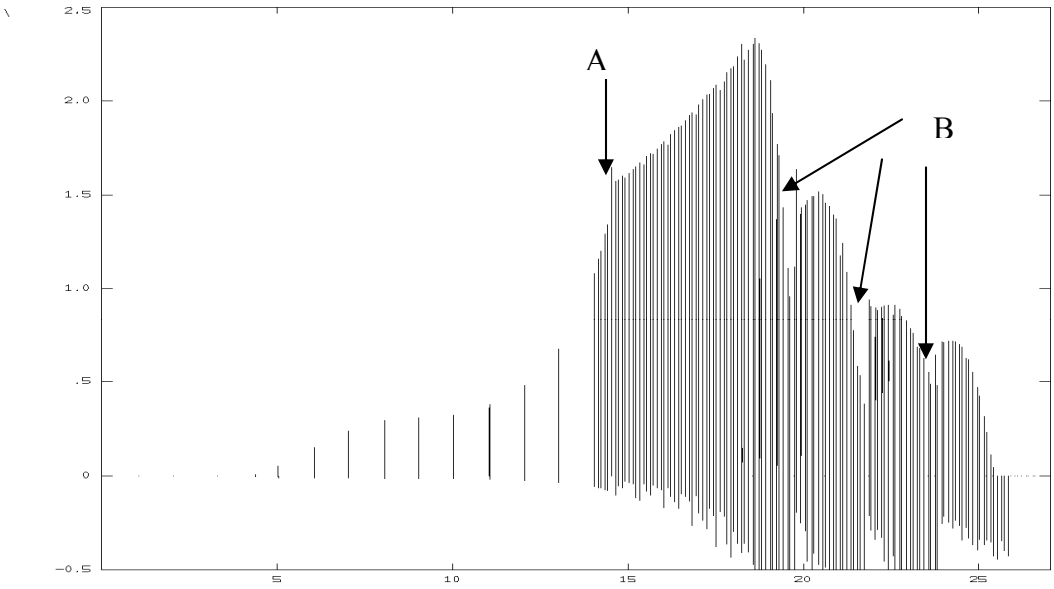

Figure 17. The stator-armature voltage difference shown with the time across and value up. Point A is the arrival of the armature at the first winding of the stator. Points B are the bifurcations in the FCG winding.

Figures 16 and 17 show the actual voltage difference between the stator and the armature. So the maximum is about 28 KV, much smaller than the source voltage. The time of the maximum is about 18 μs, and that compares well with the time of the maximum of the source voltage. So the losses are important.

When the armature-stator voltage is divided by the distance between them, one gets the average electric field magnitude, and that is shown in figures 18 and 19. Note that the peak value is about 280 KV/cm or about 28 KV/mm. The application of the enhancement factor will increase this value. So it is quite likely that this design of FCG will breakdown electrically between the armature and the stator at 18 μs or before. The remaining averages will be shown below with the enhancement factors applied.

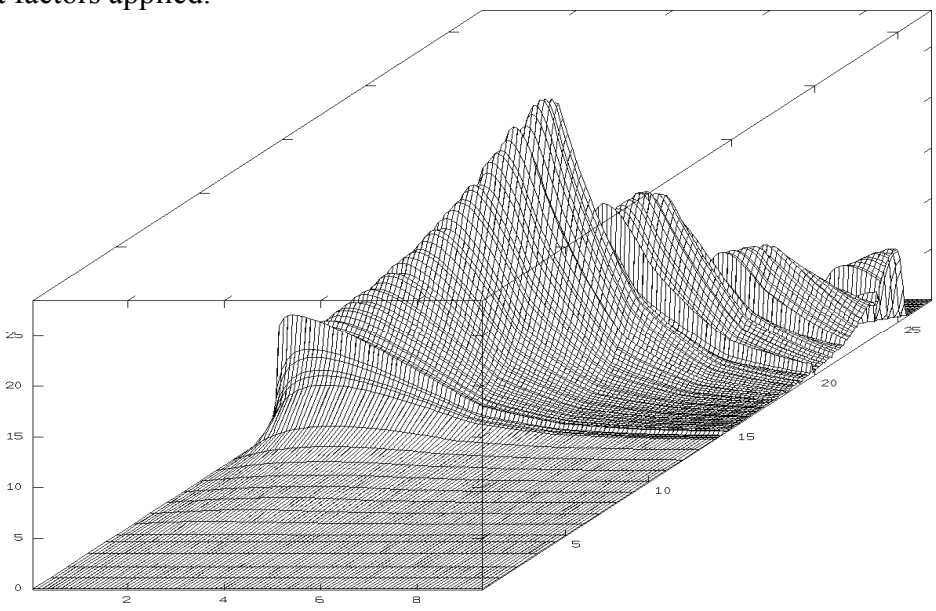

Figure 18. Shown is the average electric field between the stator and the armature. The axis in front (left-right) is the Z position down the axis of the FCG; the vertical axis is the electric field value in DKV/cm (KV/mm); and the axis into the paper is time in μs.

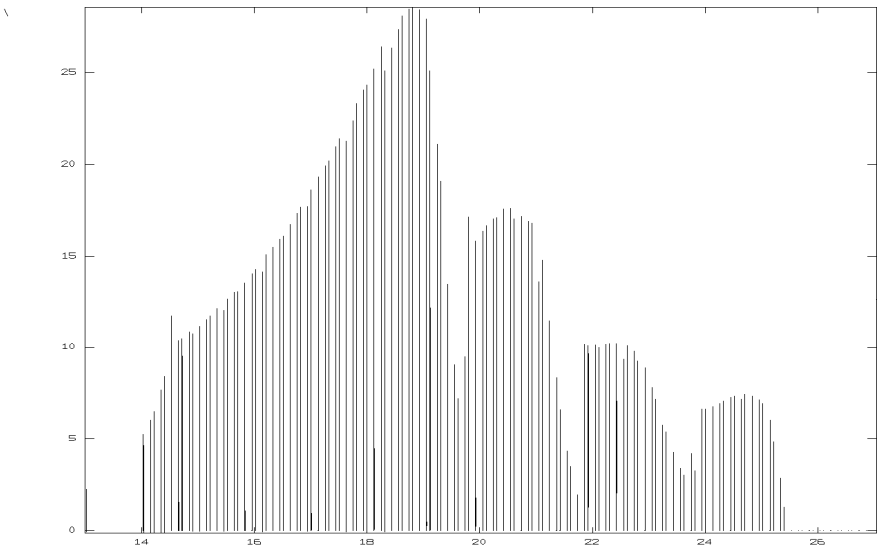

Figure 19. Shown is the value-time view of the average electric field between the stator and the armature. The axis in front (left-right) is the time; the vertical axis is the electric field value in DKV/cm (KV/mm).

3.3 THE ENHANCEMENT FACTORS

Figure 20 shows the magnitude of the electrostatic electric field between the armature and the stator measured at a selected point in front of the contact point as computed by FlexPDE. The peak value at the surface of the wire at the point nearest to the armature is seen to be 1.011E+7 Volts/meter. That number is 10.1 kV/mm and is therefore, as discussed before, in the range to cause electrical breakdown.

Figure 21 shows the inductive E field due to the time rate of change of the magnetic field in the system. The largest value is about 900 Volts/meter or less than 1 volt/mm, nearly negligible. Consequently, for this particular problem, the tendency to breakdown between the windings and the armature is nearly entirely due to the electrostatic field.

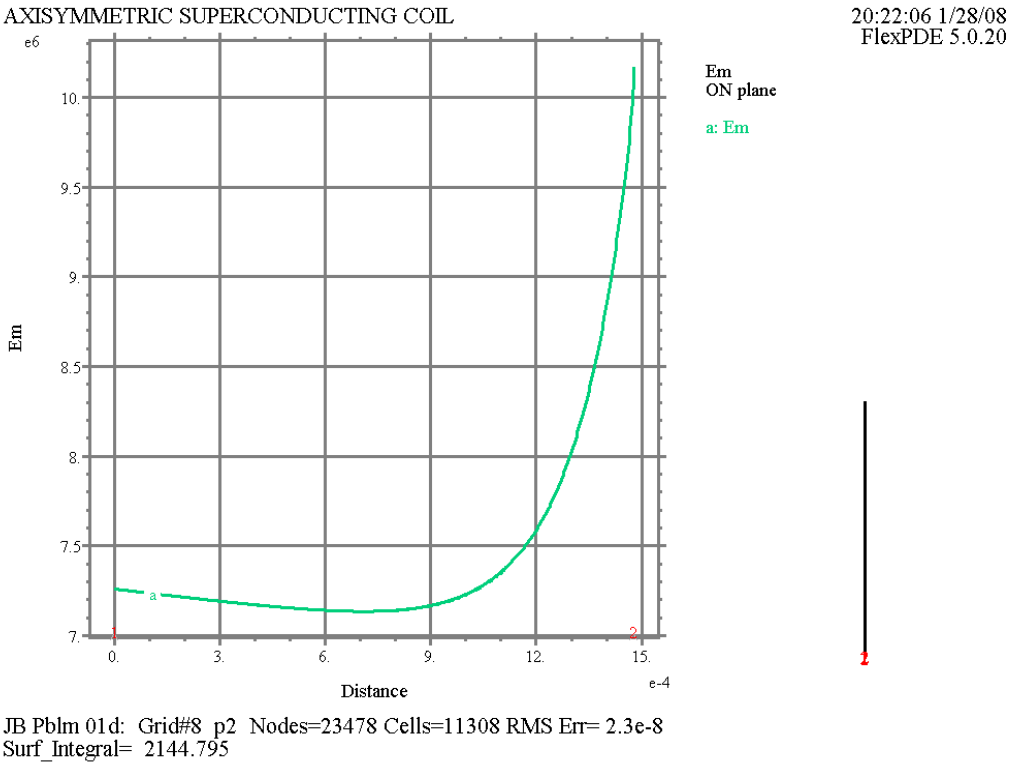

Figure 20. This plot is from FlexPDE and shows the E field along a radial path from the armature to the stator. The units are MKS. The largest value is about 10.1 kV/mm.

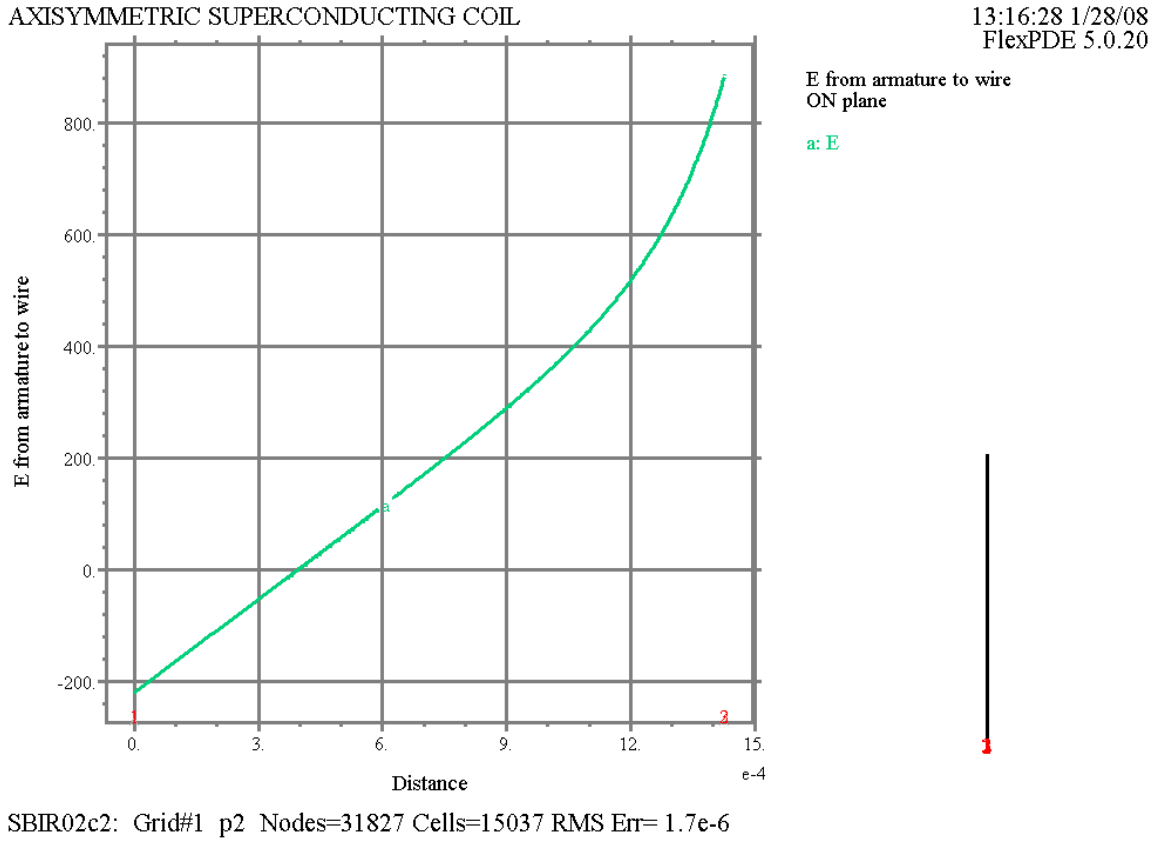

Figure 21. This plot is from FlexPDE and shows the inductive E field along a radial path from the armature to the stator. The units are MKS, and the largest value is about 900 volts/meter.

There is one additional part to the total E field description of this 2D model of the helical flux compression generator. That is the electric field due to the turn-to-turn voltage difference. It is simply the integral of the surface current density times the surface resistivity over the length of one winding circumference. The result is a voltage difference of 180.6 volts. So the average turn-to-turn E field magnitude is only about 1.2 kV/mm and is insignificant in relation to the electrostatic armature to stator field.

Thus, we have one element of a possibly 27-element matrix filled in.

Table 1. Parameters specific to the reported HGWL1 calculation.

R stator	3.2262 cm
R armature	3.0272 cm
R wire	0.0512 cm
Pitch	0.1175 cm
Volt armature to stator	11.0 kV
Volt turn to turn	0.181 kV
Max E armature to stator	10.1 kV/mm
Max E turn to turn	1.2 kV/mm
Max E inductive	0.0009 kV/mm

While the initial parameter set was taken from an actual HFCG, the final set is shown in table 2. In order to predict the maximum electric field for any HFCG, variations of the three different parameters forming the independent set for the computation of the enhancement factors are needed.

"fp" is the packing fraction: the diameter of the metal of the winding wire divided by the center-to-center spacing.

"fa" is the ratio of the armature diameter (at the local position) to the diameter of the stator (inside of the winding).

"fw" is the ratio of the winding wire diameter to the stator diameter (inside of the winding).

The dependant result is "fPE" and is the ratio of the peak electric field magnitude found to the average electric field, the enhancement factor. The average electric field magnitude is just the potential difference between the armature and the stator divided by the separation between the two.

Table 2. The range of the parameters that are used for the enhancement factor for CAGEN.

values of fw=	0.01	0.02	0.05
fa=0.5	fp=0.5, 0.8, 0.9, 0.95	fp=0.5, 0.8, 0.9, 0.95	fp=0.5, 0.8, 0.9, 0.95
fa=0.8	fp=0.5, 0.8, 0.9, 0.95	fp=0.5, 0.8, 0.9, 0.95	fp=0.5, 0.8, 0.9, 0.95
fa=0.9	fp=0.5, 0.8, 0.9, 0.95	fp=0.5, 0.8, 0.9, 0.95	fp=0.5, 0.8, 0.9, 0.95
fa=0.95	fp=0.5, 0.8, 0.9, 0.95	fp=0.5, 0.8, 0.9, 0.95	fp=0.5, 0.8, 0.9, 0.95

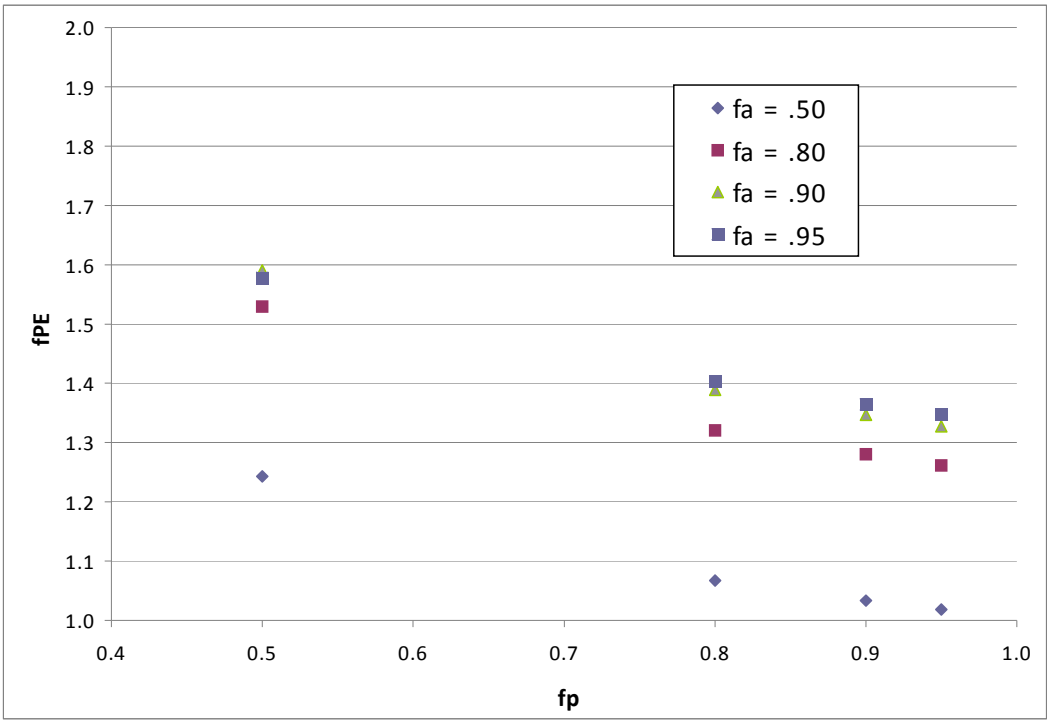

Figure 22. Shows the enhancement factor for a fixed value of the parameter **fw=0.01**. The abscissa is the packing fraction, fp. The four individual curves are for different values of fa.

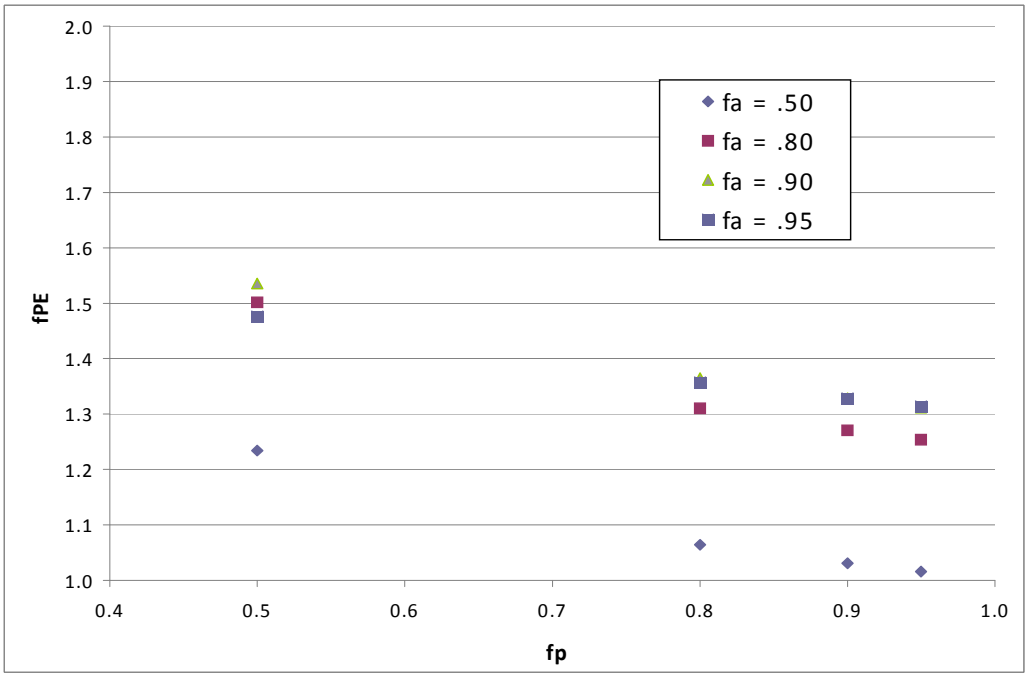

Figure 23. Shows the enhancement factor for a fixed value of the parameter **fw=0.02**. The abscissa is the packing fraction, fp. The four individual curves are for different values of fa.

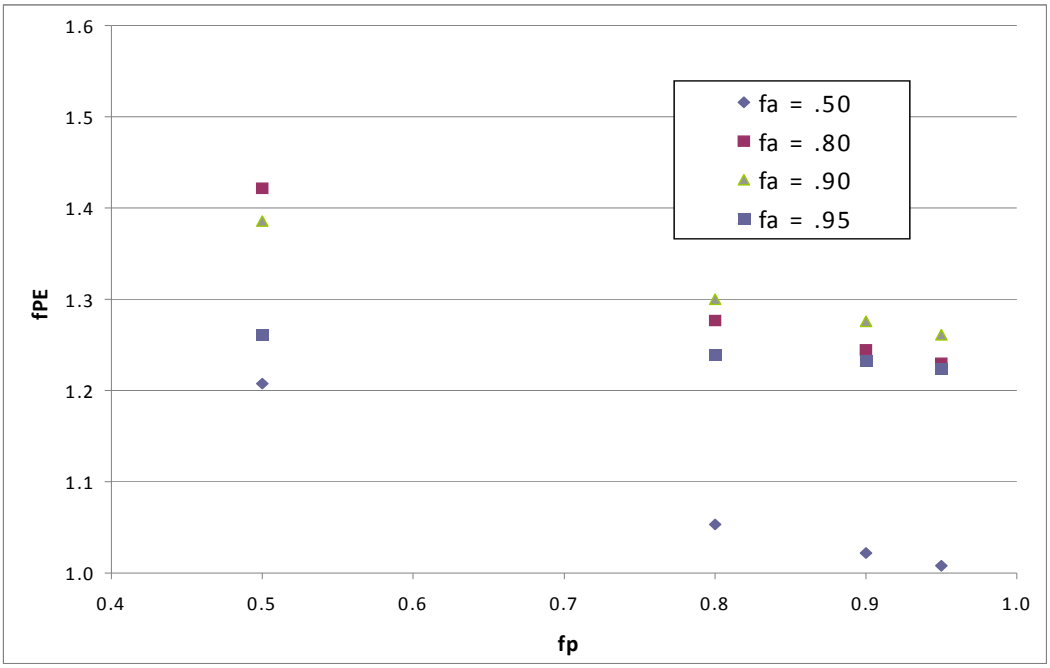

Figure 24. Shows the enhancement factor for a fixed value of the parameter **fw=0.05**. The abscissa is the packing fraction, fp. The four individual curves are for different values of fa.

3.4 CAGEN, WITH ENHANCEMENT FACTORS APPLIED RESULTS AND DISCUSSION

Calculations on CAGEN have been completed for three example helical flux compression generators (HFCG). The first is the original HFCG that acted as the baseline for the project. It was called HGWL1. It is quite small, only 80 mm in diameter, and is a model of an HFCG that electrically broke down. The second, called HHT79, is a very large HFCG, more than 300 mm in diameter, and it did not break down. The third HFCG is called JAKE and is 170 mm in diameter. It has been known to break down electrically, but the results of an experiment are not available.

All three of the included examples, HGWL1, HHT79, and JAKE, use insulation around the wires used for the stator winding. Some use layers of insulation layered against the cylindrical inside surface of the windings, as well. All three of these HFCG designs use gaseous SF_6at one atmosphere of pressure to fill the volume between the armature and the stator. Consequently, knowing the electric field strength everywhere within the HFCG will not determine the probability of electrical breakdown. There are generally accepted danger zones. For example, in dry air one would expect breakdown to occur at about 1 kV/mm, while in one atmosphere of SF_6that value might be as much 4 kV/mm, and most common solid insulators begin to break at 20 kV/mm. However, with the knowledge of how large and where the electric field maxima are located, for systems with similar materials, predictions can begin to be made. This work provides the first portion of the set of knowledge that is required. This work enables the prediction of the electric field structure.

Figures 25 and 26 show the voltage within the small HFCG, HGWL1, as a function of axial position and time. The first view is in perspective while the second shows the maxima versus time. From the second, the voltage maximum can be determined. Marked on this plot is the

approximate time of the experimental electric breakdown. This would suggest that the maximum voltage at that time was 17-18 kV. Of course, it is not voltage that causes breakdown, it is the *electric field strength*. Figures 27 and 28 show the electric field maximum that appears between the armature and the stator, including enhancements, as a function of axial position and time. Usually the maximum will be near the stator-winding surface (that is, assuming the stator wire enhancement dominates the intrinsic 1/r general scaling). In figure 28, one can see that the E field magnitude at 16 μs is about 20 kV/mm. That is certainly in the region where solid dielectrics begin to break.

Figure sets 29-32 and 33-36 are similar but for larger HFCGs. The design HHT79 is more than 320 mm in diameter, and the JAKE is about 170 mm in diameter. These are to be compared with the HGWL1 at about 80 mm in diameter. Each of these device designs can be made to fail, electrically, by injecting ever-larger initial currents at the beginning of their explosive operation. As shown in the figures, all of these larger designs have much lower peak electric field magnitudes. HHT79 has about 6 kV/mm, and JAKE is below 15 kV/mm. Both are considerably below that exhibited by HGWL1. While JAKE might be close to some threshold of breakdown, HHT79 is comfortably far from any disaster from electrical breakdown. Recognizing these traits and taking advantage of them by adjusting designs is the *raison d'etre* of this project.

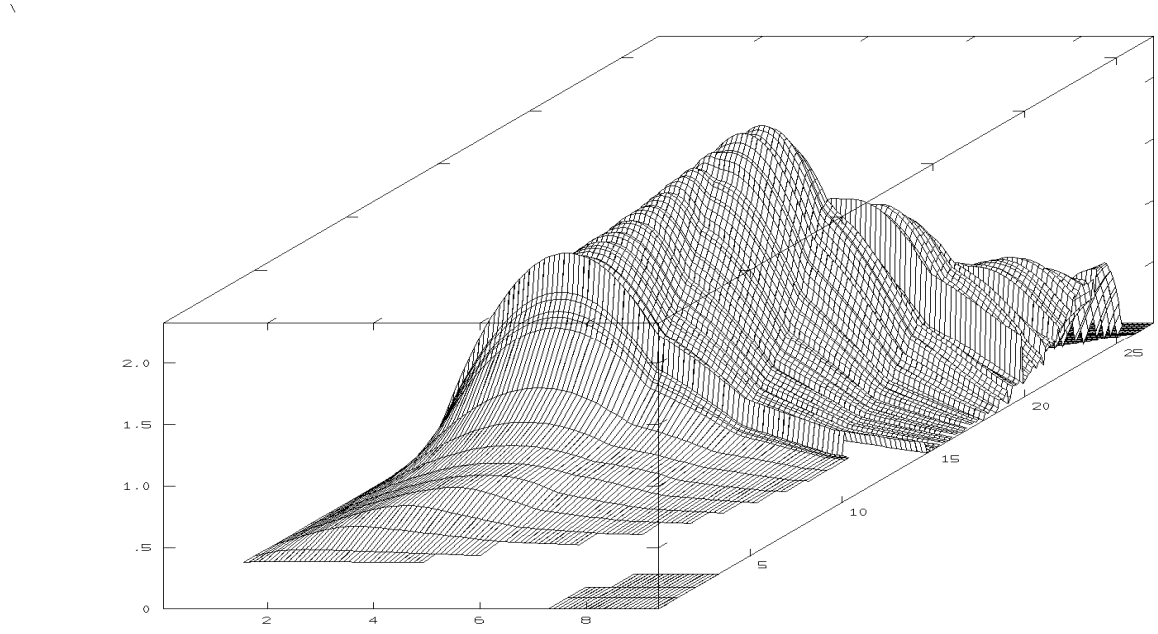

Figure 25. This is the voltage between the armature and the stator windings for the problem HGWL1. The abscissa is the distance along the axis of the HFCG. The ordinate is the value of the voltage in DKV (1.0E4 Volts), and the axis into the paper is the time in μs

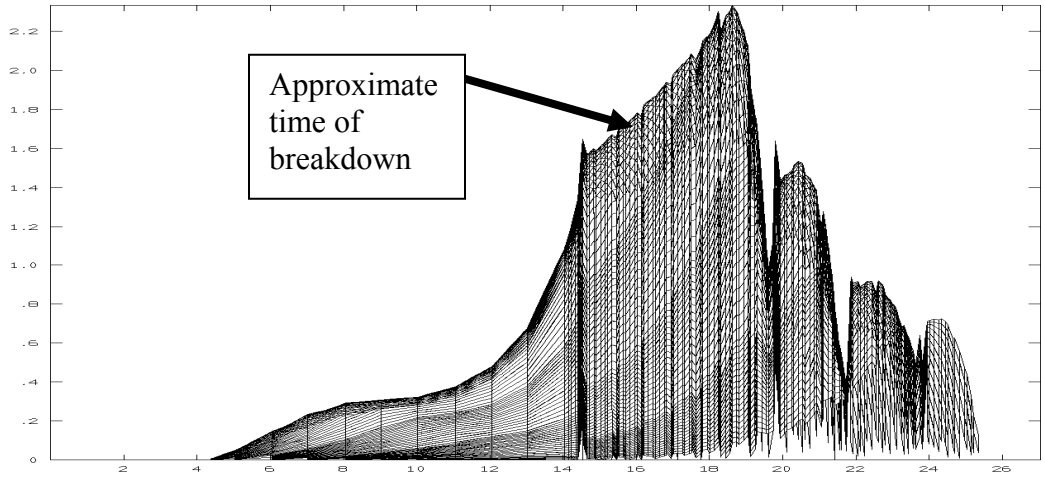

Figure 26. This is the voltage between the armature and the stator windings for the problem HGWL1. The abscissa is the time in μs. The ordinate is the value of the voltage in DKV (1.0E4 Volts), and the axis into the paper (not in view) is the distance along the axis of the HFCG. This is another view of Figure 25. Note: the maximum of the voltage is about 23 kV and happens at 18.5 μs.

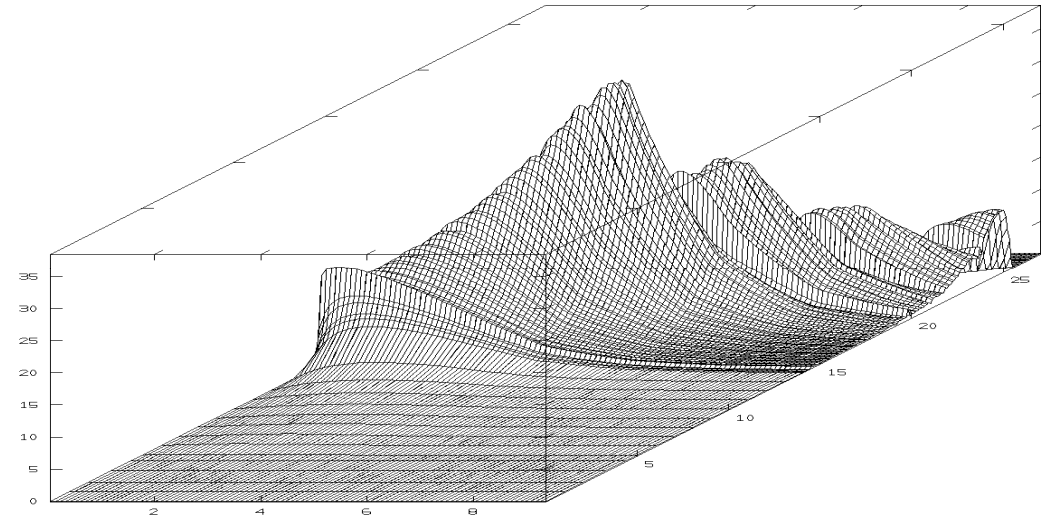

Figure 27. This is the maximum electric field magnitude found between the armature and the stator windings for the problem HGWL1. The abscissa is the distance along the axis of the HFCG. The ordinate is the value of the electric field in DKV/cm (1.0E4 Volts/cm = kV/mm), and the axis into the paper is the time in μs.

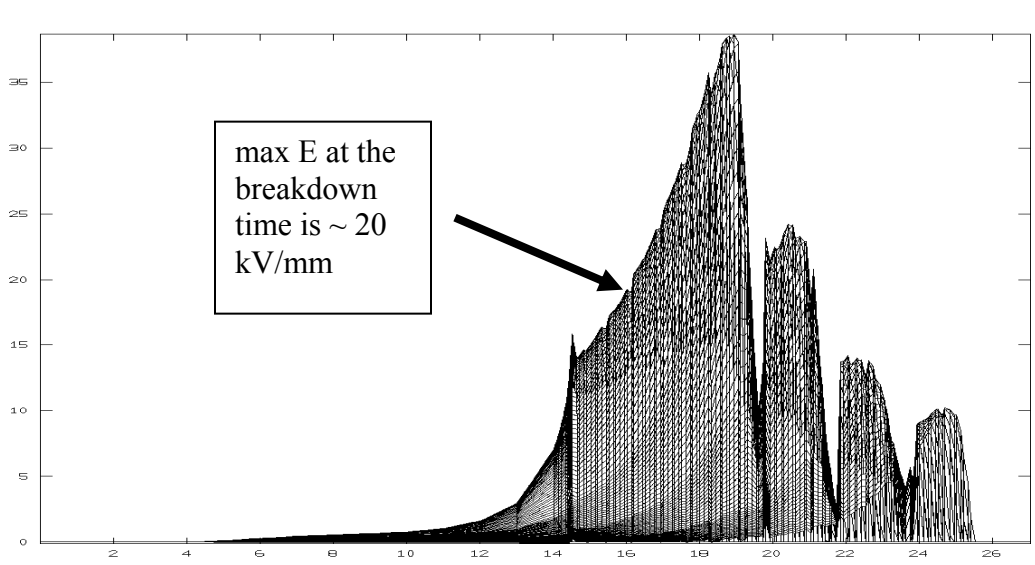

Figure 28. This is the maximum electric field magnitude found between the armature and the stator windings for the problem HGWL1. The abscissa is the time in μs. The ordinate is the value of the electric field in DKV/cm (1.0E4 Volts/cm = kV/mm), and the axis into the paper (not in view) is the distance along the axis of the HFCG. This is another view of Figure 27. Note: the maximum of the field anywhere is about 380 kV/cm and happens at 18.8 μs.

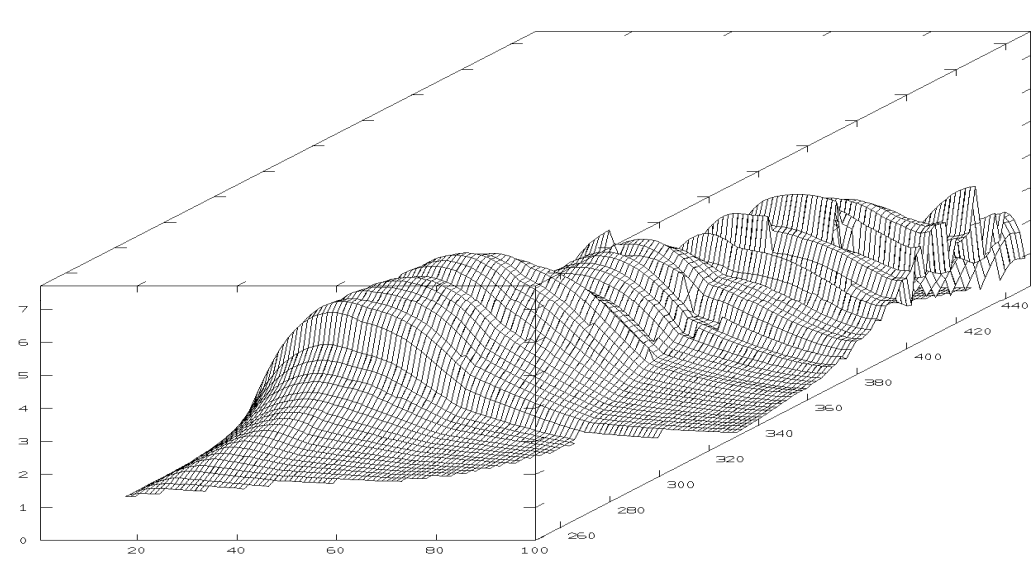

Figure 29. This is the voltage between the armature and the stator windings for the problem HHT79. The abscissa is the distance along the axis of the HFCG. The ordinate is the value of the voltage in DKV (1.0E4 Volts), and the axis into the paper is the time in μs.

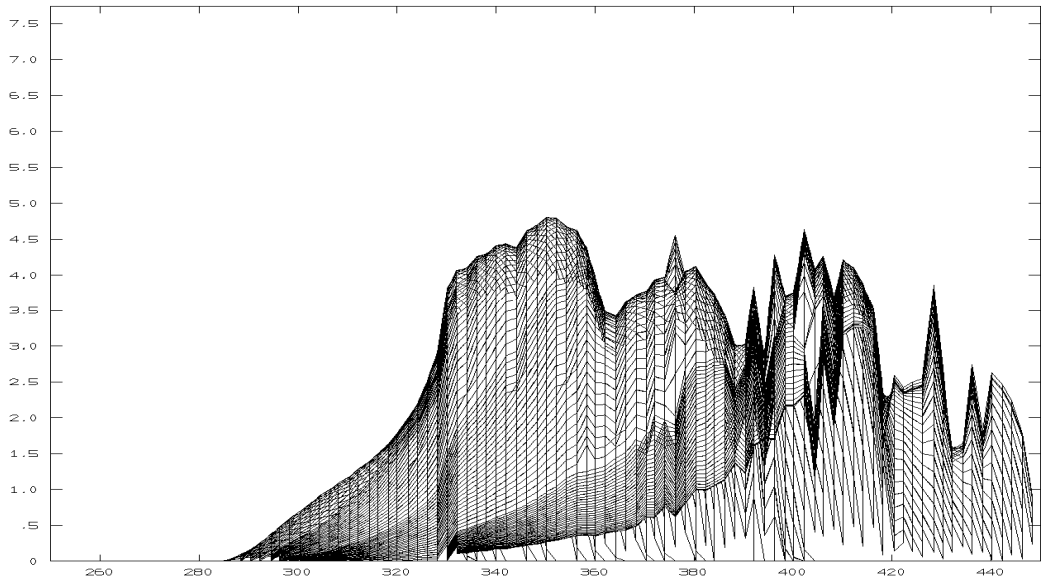

Figure 30. This is the voltage between the armature and the stator windings for the problem HHT79. The abscissa is the time in μs. The ordinate is the value of the voltage in DKV (1.0E4 Volts), and the axis into the paper (not in view) is the distance along the axis of the HFCG. This is another view of Figure 29. Note: the maximum of the voltage is about 48 kV and occurs at 360 μs.

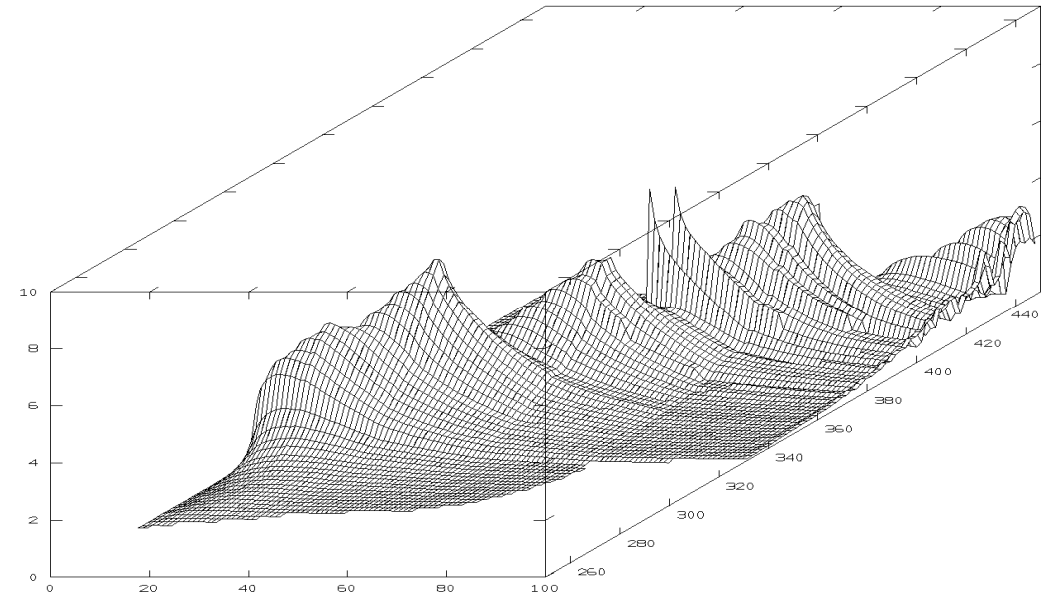

Figure 31. This is the maximum electric field magnitude found between the armature and the stator windings for the problem HHT79. The abscissa is the distance along the axis of the HFCG. The ordinate is the value of the electric field in DKV/cm (1.0E4 Volts/cm = kV/mm), and the axis into the paper is the time in μs.

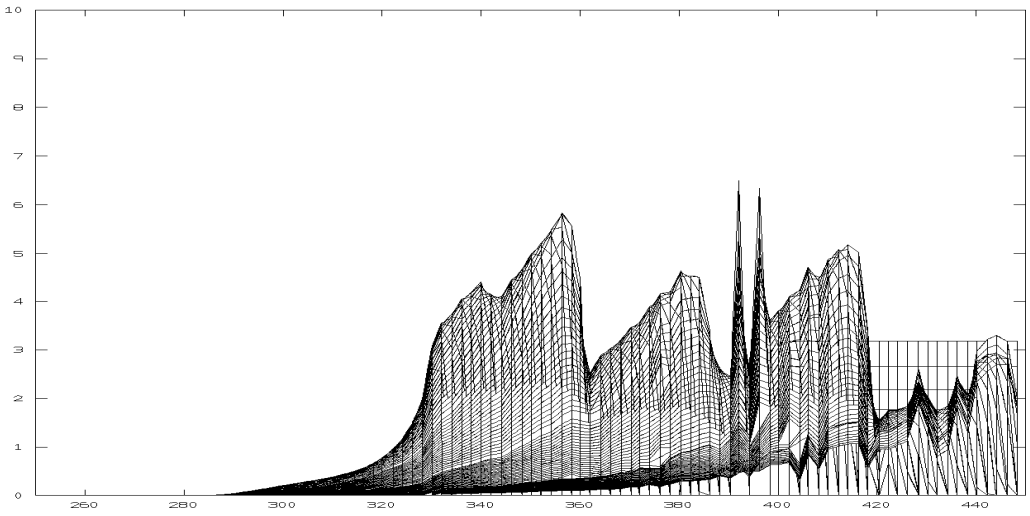

Figure 32. This is the maximum electric field magnitude found between the armature and the stator windings for the problem HHT79. The abscissa is the time in μs. The ordinate is the value of the electric field in DKV/cm (1.0E4 Volts/cm = kV/mm), and the axis into the paper (not in view) is the distance along the axis of the HFCG. This is another view of Figure 31. Note: the maximum of the field is about 60 kV/cm and happens at about 349 μs.

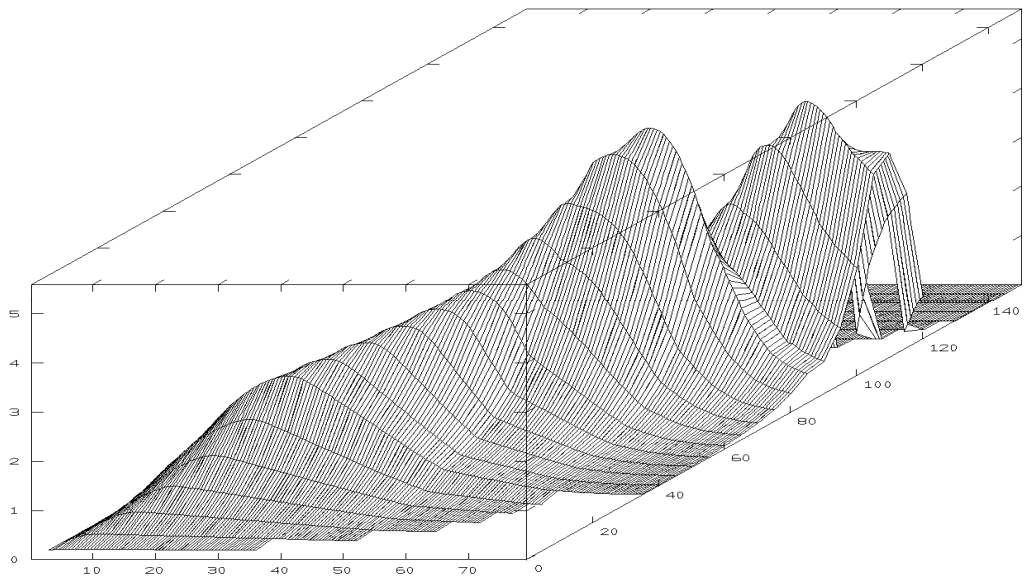

Figure 33. This is the voltage between the armature and the stator windings for the problem JAKE. The abscissa is the distance along the axis of the HFCG. The ordinate is the value of the voltage in DKV (1.0E4 Volts), and the axis into the paper is the time in μs

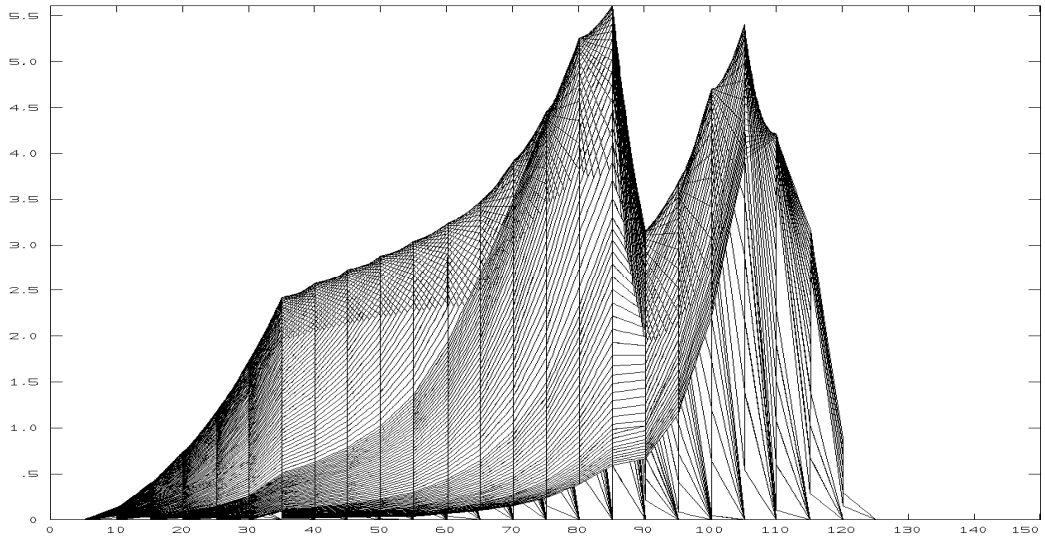

Figure 34. This is the voltage between the armature and the stator windings for the problem JAKE. The abscissa is the time in μs. The ordinate is the value of the voltage in DKV (1.0E4 Volts), and the axis into the paper (not in view) is the distance along the axis of the HFCG. This is another view of Figure 33. The maximum voltage is 66 kV and occurs at 85 μs.

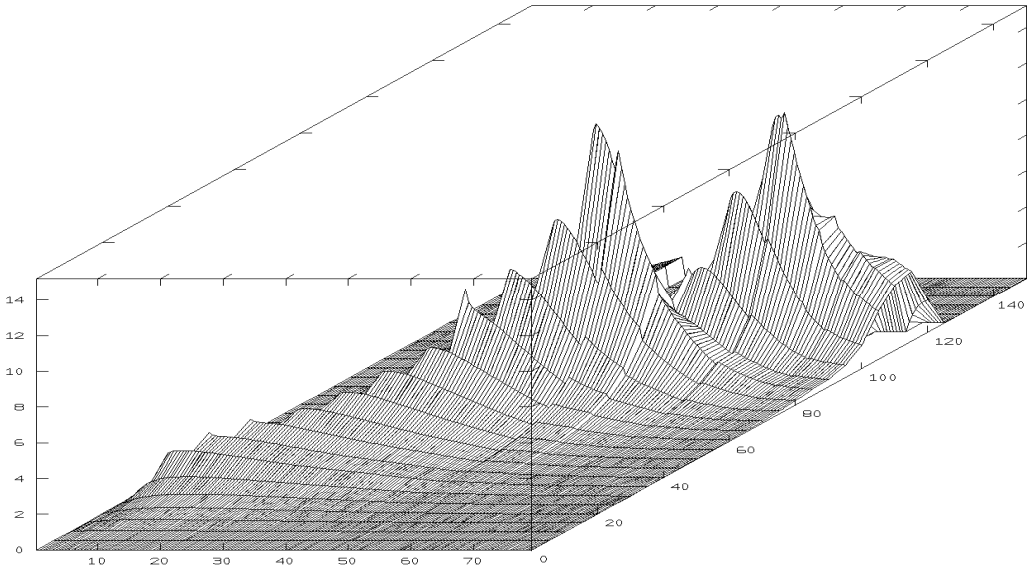

Figure 35. This is the maximum electric field magnitude found between the armature and the stator windings for the problem JAKE. The abscissa is the distance along the axis of the HFCG. The ordinate is the value of the electric field in DKV/cm (1.0E4 Volts/cm = kV/mm), and the axis into the paper is the time in μs.

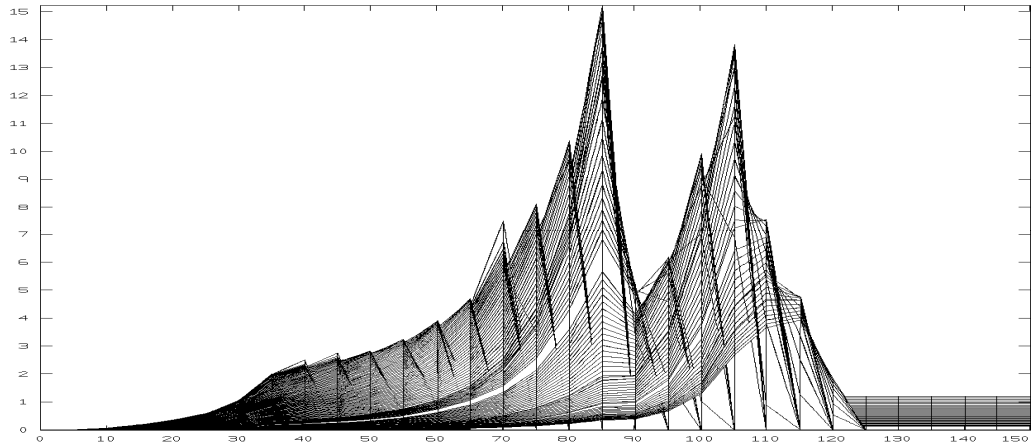

Figure 36. This is the maximum electric field magnitude found between the armature and the stator windings for the problem JAKE. The abscissa is the time in μs. The ordinate is the value of the electric field in DKV/cm (1.0E4 Volts/cm = kV/mm), and the axis into the paper (not in view) is the distance along the axis of the HFCG. This is another view of Figure 35. Note: the maximum of the field is about 150 kV/cm and happens at about 85 μs.

4.0 CONCLUSIONS

We have achieved the last of our goals: the complete inclusion in the model code CAGEN for predicting the electric fields within an explosively powered helical flux compression generator. We accomplished this task by using purely two-dimensional physics equation solutions from the trademarked code FlexPDE.

The development of the 3D helical model has been pursued with the notion that some benchmarking of the three dimensional limitations to our models would be wise. However, nothing was developed within the time span of the project lifetime.

5.0 REFERENCES

1. G. F. Kiuttu and J. B. Chase, “An armature-stator contact resistance model for explosively driven helical magnetic flux compression generators,” Proc. 15th IEEE Intl. Pulsed Power Conf., Monterey (2005).

2. J. B. Chase, D. Chato, G. Peterson, and G. F. Kiuttu, “Benchmarking the Care’n Co. flux compression generator code, CAGEN, implementing the Kiuttu contact resistance model,” 15th Intl. Pulsed Power Conf., Monterey (2005).

3. G. F. Kiuttu, J. B. Chase, D. M. Chato, and G. Peterson, “Recent advances in modeling helical FCGs,” Proc. Megagauss 2006, Santa Fe (2006) (to be published).

4. J. B. Chase, G. F. Kiuttu, G. Peterson, and D. M. Chato, “Twenty-five years of helical flux compression generator modeling leading to the current code CAGEN,” Proc. Megagauss XI, London, 5-9 September 2006 (to be published).

5. J. V. Parker, T. C. Cavazos, C. E. Roth, J. H. Degnan, G. F. Kiuttu, F. M. Lehr, and S. K. Coffey, “Development and testing of a high-gain magnetic flux compression generator,” Proc. Megagauss 2006, Santa Fe (2006) (to be published).

6. W. Atchison, LANL, private communication, 2006.

7. G. F. Kiuttu, “Calculation of inductive electric fields in high-current pulsed devices using electric vector potentials,” Proc. 13th IEEE Intl. Pulsed Power Conf., R. Reinovsky and M. Newton, eds., IEEE (2001), pp. 1506–1508.

8. J. B. Chase, "CIRC: A specialized circuit analysis computer simulation program for a high explosive generator model," in *Megagauss Technology and Pulsed Power Applications*, C. M. Fowler, R. S. Caird, and D. J. Erickson, eds., Plenum Press, New York (1987), pp. 397–404.

9. D. K. Abe and J. B. Chase, "Experiments with small helical flux compression generators,” in *Megagauss Technology and Pulsed Power Applications*, C. M. Fowler, R. S. Caird, and D. J. Erickson, eds., Plenum Press, New York (1987), pp. 405–410.

10. D. K. Abe and J. B. Chase, "Comparison of numerical helical generator simulations with experimental results,” in *Megagauss Physics and Technology*, P. J. Turchi, ed., Plenum Press, New York (1980), pp. 411–416.

11. P. A. Pincosy, J. L. Cutting, and J. B. Chase, “Testing and performance of a high-gain flux-compression generator,” in *Megagauss Fields and Pulsed Power Systems*, V.M. Titov and G.A. Shvetsov, eds., Nova Science Publishers, New York (1990), pp. 411–418.

12. J. B. Chase, D. Chato, G. Peterson, and P. Pincosy, “CAGEN: A Modern, PC-based computer modeling tool For explosive MCG generators and attached loads,” Proc. 11th IEEE Intl. Pulsed Power Conf., IEEE, (1997), pp. 1005–1009.

13. J. B. Chase, D. Chato, G. Peterson, P. Pincosy, and G. F. Kiuttu, "CAGEN: A modern PC based computer modeling tool for explosive MCG generators and attached loads," Proc. 12th IEEE Intl. Pulsed Power Conf., C. Stallings and H. Kirbie, eds., IEEE (1999), pp. 597–600.

APPENDIX A

The Work Breakdown Structure

The work breakdown structure shown in table A-1, has evolved over the course of the project. The major change was the elimination of tasks 1.3.1 (1.3.1.1 and 1.3.1.2) because the technical work in 1.3.3 showed that the conjectures implied in 1.3.1 were not even necessary to explain the data in hand, and were probably wrong.

Table A-1. The Work Breakdown Structure of this project.

WBS Level	Task Name	Duration (days)	Start Date	End Date	Predecessor
1	HV FCG Analysis	173	05/14/07	01/09/08	
1.1	Contract Award	0	05/14/07	05/14/07	
1.2	Kickoff Meeting	6	05/29/07	06/05/07	1.1
1.3	Evaluate Issues	50	06/05/07	08/14/07	1.2
1.3.1	Hydro Issues	33	06/05/07	07/20/07	1.2
1.3.1.1	SF6 EOS	15	06/05/07	06/26/07	1.2
1.3.1.2	Jetting Calcs	18	06/26/07	07/20/07	1.3.1.1
1.3.2	v x B Calcs	12	07/20/07	08/07/07	1.3.1.2
1.3.3	Electrical Issues	50	06/05/07	08/14/07	1.2
1.3.3.1	Poloidal E Calcs	25	06/05/07	11/01/07	1.2
1.3.3.2	Toroidal E Calcs	25	07/10/07	11/01/07	1.3.3.1
1.4	CAGEN Implementations	25	11/01/07	12/01/07	1.3
1.5	Intermediate Report Prep	15	09/18/07	10/01/07	1.4
1.6	Intermediate Review	3	10/01/07	10/04/07	1.5
1.7	Advanced Analysis	48	11/01/07	01/01/08	1.6
1.8	Final Report Prep	23	12/11/07	01/06/08	1.7
1.9	Final Review	3	01/07/08	01/09/08	1.8
2	Monthly status reports	175	06/13/07	02/13/08	
2.1	Monthly status reports 1	0.25	06/13/07	06/13/07	
2.2	Monthly status reports 2	0.25	07/13/07	07/13/07	
2.3	Monthly status reports 3	0.25	08/13/07	08/13/07	
2.4	Monthly status reports 4	0.25	09/13/07	09/13/07	
2.5	Monthly status reports 5	0.25	10/13/07	10/13/07	
2.6	Monthly status reports 6	0.25	11/13/07	11/13/07	
2.7	Monthly status reports 7	0.25	12/13/07	12/13/07	
2.8	Monthly status reports 8	0.25	01/13/08	01/13/08	
2.9	Monthly status reports 9	0.25	02/13/08	02/13/08	

DISTRIBUTION LIST

DTIC/OCP
8725 John J. Kingman Rd, Suite 0944
Ft Belvoir, VA 22060-6218 1 cy

AFRL/RVIL
Kirtland AFB, NM 87117-5776 2 cys

Care'n LLC
12137 Midway Drive, Tracy, CA 95377 1 cy

Official Record Copy
AFRL/RDHP/Tyrone Tran 1 cy

This Page Intentionally Left Blank